HHS Public Access

Author manuscript

J Mol Cell Cardiol. Author manuscript; available in PMC 2021 June 29.

Published in final edited form as:

J Mol Cell Cardiol. 2021 June ; 155: 112–124. doi:10.1016/j.yjmcc.2021.02.009.

The Effect of Variable Troponin C Mutation Thin Filament Incorporation on Cardiac Muscle Twitch Contractions

Srboljub M. Mijailovich[1,*], **Momcilo Prodanovic**[2,3], **Corrado Poggesi**[4], **Joseph D. Powers**[5,6], **Jennifer Davis**[5], **Michael A. Geeves**[7], **Michael Regnier**[5]

[1]Dept. of Biological Sciences, Illinois Institute of Technology, Chicago, IL 60616

[2]Bioengineering Research and Development Center (BioIRC), 34000 Kragujevac, Serbia

[3]Faculty of Engineering, University of Kragujevac, 34000 Kragujevac, Serbia

[4]Department of Experimental & Clinical Medicine, University of Florence, Florence 50134, Italy

[5]Department of Bioengineering, University of Washington, Seattle, WA 98105, USA

[6]Dept. of Bioengineering, University of California San Diego, CA 92093

[7]Dept. of Biosciences, University of Kent, Canterbury, Kent CT2 7NJ, UK

Abstract

One of the complexities of understanding the pathology of familial forms of cardiac diseases is the level of mutation incorporation in sarcomeres. Computational models of the sarcomere that are spatially explicit offer an approach to study aspects of mutational incorporation into myofilaments that are more challenging to get experimentally. We studied two well characterized mutations of cardiac TnC, L48Q and I61Q, that decrease or increase the release rate of Ca^{2+} from cTnC, k_{-Ca}, resulting in HCM and DCM respectively [1]. Expression of these mutations in transgenic mice was used to provide experimental data which showed incorporation of 30 and 50% (respectively) into sarcomeres. Here we demonstrate that fixed length twitch contractions of trabeculae from mice containing mutant differ from WT; L48Q trabeculae have slower relaxation while I61Q trabeculae have markedly reduced peak tension. Using our multiscale modelling approach [2] we were able to describe the tension transients of WT mouse myocardium. Tension transients for the mutant cTnCs were simulated with changes in k_{-Ca}, measured experimentally for each cTnC mutant in whole troponin complex, a change in the affinity of cTnC for cTnI, and a reduction in the number of detached crossbridges available for binding. A major advantage of the multiscale explicit 3-D model is that it predicts the effects of variable mutation incorporation, and the effects of variations in mutation distribution within thin filaments in sarcomeres. Such effects are currently impossible to explore experimentally. We explored random and clustered distributions of

[*]Corresponding author at: Srboljub M. Mijailovich Illinois Institute of Technology Department of Biology 182C Robert A. Pritzker Science Center Chicago, IL 60616 smijailo@gmail.com.

Conflict of Interest: This article reflects only the author's view. The European Commission is not responsible for any use that may be made of the information it contains.

mutant cTnCs in thin filaments, as well as distributions of individual thin filaments with only WT or mutant cTnCs present. The effects of variable amounts of incorporation and non-random distribution of mutant cTnCs are more marked for I61Q than L48Q cTnC. We conclude that this approach can be effective for study on mutations in multiple proteins of the sarcomere.

Summary—A challenge in experimental studies of diseases is accounting for the effect of variable mutation incorporation into myofilaments. Here we use a spatially explicit computational approach, informed by experimental data from transgenic mice expressing one of two mutations in cardiac Troponin C that increase or decrease calcium sensitivity. We demonstrate that the model can accurately describe twitch contractions for the data and go on to explore the effect of variable mutant incorporation and localization on simulated cardiac muscle twitches.

Keywords

computational model; simulations; troponin C mutation; cardiac; twitch kinetics; variable incorporation

1. Introduction

Cardiac muscle twitch contractions are initiated by a transient increase in intracellular calcium (Ca^{2+}), which binds to the N-terminus of the cardiac troponin C (cTnC) subunit of troponin (cTn). This increases cTnC affinity for troponin I (cTnI), allowing cTnC to compete with actin for binding the TnI. The associated reduction in cTnI interaction with actin results in increased mobility of thin filament tropomyosin, exposing myosin binding sites on actin that allows myosin-actin crossbridge formation and contraction [3]. As Ca^{2+} dissociates from cTnC, it is rapidly pumped back into the sarcoplasmic reticulum or extruded from cardiomyocytes via protein pumps and ion exchangers. Without bound Ca^{2+}, cTnC affinity for cTnI is reduced and, in turn, cTnI affinity for actin is increased, reducing tropomyosin mobility, and allowing the reduction of force and relaxation. Amino acid variations (mutations) in cTn subunits, like those associated with hypertrophic or dilated cardiomyopathy (HCM and DCM, respectively), often affect the Ca^{2+} binding to cTnC. In turn, this affects the Ca^{2+} sensitivity of myofibril force development and the dynamics of contractile activation and relaxation [4]. These changes can be progressive as the level of mutational incorporation (i.e., variant expression levels) in sarcomeres increases as shown in *in-vitro* studies with TnC [5] and in transgenic mice. It should be noted, however, that the situation with TnT mutations is more complex [6]. Determining how variable mutational incorporation affects cardiac twitch contractions, and the onset and progression of cardiac disease are important questions that have not been well studied.

The most commonly used methods for studying how cTn mutations affect contractile properties have been to measure the steady-state force or the kinetics of force redevelopment (following transient length changes) as a function of [Ca^{2+}] in demembranated cardiac muscle tissue or the activation and relaxation dynamics with isolated sub-cellular contractile organelles (myofibrils) via rapid Ca^{2+} solution switching [7, 8]. For some studies, native cTn has been exchanged (via mass action) with recombinant cTn complexes containing the mutation of interest in either cTnC, cTnI or cTnT. Most of these studies have reported on the effects of 100% exchange with the mutation (or as close to this as possible) [9]. However, in

cardiac muscle from patients, or transgenic animal models, the incorporation of a mutation into sarcomeres is substantially less than 100%. Variable mutant troponin expression in animal models of disease is reported by linking the fraction of troponin mutant incorporation to severity of muscle functional change. For example incorporation of ≈21% of mutant $cTnC^{A8V}$ into the cardiac myofilament reduced diastolic sarcomeric length, increased shortening, prolonged Ca^{2+} and contractile transients [10], similar to changes observed due to 30% incorporation of $cTnC^{I61Q}$ in transgenic mice [1]. The dose dependent incorporation of $cTnT^{R92Q}$ affects cardiac muscle hypercontractility but shows mild or no ventricular hypotrophy [11] and incorporation of 43% $cTnT^{179N}$ causes not only change HCM features such as sarcomere disorganization, increase in systolic contractility and impaired relaxation but also the pro-arrhythmic changes of the human ventricular action potential [12]. Likewise the incorporation of ~25% $cTnI^{R21C}$ within the myofilament virtually abolishes $cTnI^{R21C}$ phosphorylation and this dose of the mutation is sufficient to develop a notable degree of cardiac hypertrophy and fibrosis in mutant mice [13]. Taken together, the observed changes in the contractile properties, tension Ca^{2+} sensitivity and structural changes in heart walls from these specifically designed animal model preparations may not accurately predict the twitch behavior of patient cardiac tissue, due to neuro-humoral adaptive responses and patient treatment regimens.

Multiscale computational models can help overcome these experimental and analytic complexities, without the need for multiple types of experiments and protocols, especially when tissue availability is limited. We recently reported on the development of a multiscale model that effectively simulates the force dynamics of rat cardiac twitch contractions under multiple conditions, as well as the tension-Ca^{2+} relationship of cardiac muscle [2]. This model can account for internal sarcomere length changes that occur when twitches are measured in muscle fixed length conditions and also includes a ‘parked state’ of myosin (analogous to the “super-relaxed state” [14, 15]) that is essential to accurately simulate the absolute tension and kinetics of the twitch. We have now adapted this model, originally developed for rat myocardium, to simulate twitches of cardiac muscle from transgenic mice containing mutations in cTnC, to understand the mechanisms by which mutations affect contraction and relaxation.

Here we report the ability of this multiscale model approach to predict how variable amounts of two different mutant cTnC’s affect twitch contractions in cardiac muscle. We chose to study mutations affecting the binding of Ca^{2+} by cTnC and the subsequent interaction between cTnC and cTnI in the cTn complex that we [9, 16–18] and others [19] have reported. These cTnC mutations, L48Q and I61Q, have, respectively, increased and decreased Ca^{2+} binding affinity of cTnC, and Ca^{2+} and sensitivity of force in demembranated cardiac muscle (see Fig. 1 [1, 9]). They affect contraction of cardiomyocytes [20] and left ventricular function in transgenic animals [1, 21]. Thus, they present an identifiable, small set of parameters that are directly affected (with implications for function at larger scales) that can be quantitatively assessed in our sarcomere model simulations [9, 17, 18]. While these mutations have not been identified as variants in humans, our studies in transgenic mouse models demonstrate they can result in severe DCM (I61Q) and mild-moderate HCM (L48Q) in transgenic mice [1, 21]. However, while other studies in mice with long-term expression cTnCL48Q also observed higher peak twitch

tension, slower relaxation, higher fractional shortening and ejection fraction, they did not show cardiac hypertrophy [22]. To demonstrate the effect of these two cTnC mutations we initially simulated twitches of trabecula from these mice that contained 30% cTnCL48Q or 50% $cTnC^{I61Q}$, as determined by Davis et al. [1], and found that the altered Ca^{2+} binding affinity of mutant cTnC (Fig. 1B) affects time course of twitches in a predictable way. To accomplish this, the only parameters that needed to be adjusted, apart from Ca^{2+} dissociation rate (k_{-Ca}), were the affinity of cTnC for cTnI (λ), and a minor change to the rate constant for myosin detachment from actin (k^{o}_{-A}). We also investigated the effect of varying mutation incorporation and mutation clustering pattern in thin filaments on cardiac twitches. Our simulations demonstrate the potential for quantifying changes in twitch contraction that result from variable amounts of mutant incorporation and the power of structurally based computational models to examine mutation incorporation and patterns in cardiac muscle. A preliminary report of this work was published previously [23, 24].

2. Methods

2.1. Spatially explicit computational models of sarcomeres

A new generation of models considers the explicit three-dimensional (3-D) structure of a sarcomere following each interaction between sarcomere proteins, e.g., myosin with actin, the troponin-tropomyosin complex with the actin surface, and between the proteins with small molecules, e.g., Ca^{2+} [25–29]. This approach permits tracing the effects of the protein mutations on contractile characteristics of striated muscles. Earlier models which considered the 3-D explicit geometry, have used two or three state crossbridge cycles [28] coupled with models of thin filament regulation [25–27]. More detailed models consider, in addition, the effects of nonuniform distribution of actin filament lengths, changes of interfilament spacing and the effect of titin-based passive tension on overall level of activation [29].

Following these approaches, we have developed computational model for twitch contractions in intact trabecula [2]. Trabeculae are composed of longitudinally aligned myocytes. Within each myocyte there are myofibrils in parallel, and within myofibrils, there are sarcomeres in series. The 3-D sarcomere structure contains an array of thin and thick filaments connected by crossbridges and other elastic elements (e.g., titin) in a lattice structural network. Active force generation is achieved via a crossbridge cycle that converts chemical energy into mechanical energy, defined by the ATPase cycle. Myosin-actin interactions are simulated using a six-state crossbridge cycle, which contains a ‘parked state’ (PS) where myosin heads are held near the backbone of the thick filament in an ordered pattern in the so called super relaxed (SRX) state [15, 30] or in the disordered relaxed state proximate to the backbone (DRX) [14, 31]. In contrast, heads in the activated state are away from the backbone and available to interact with actin.

The PS was needed as a source for myosin recruitment during activation and a sink for de-recruitment during relaxation to achieve the kinetics of twitch contractions [2]. The definition of states in our six-state scheme are described in the supplemental material and is shown in Fig. S1. The transition rates between the crossbridge cycle states for rat cardiac trabeculae were defined in Mijailovich et al. [2] where the transition from PS into the

M.D.Pi state was modelled as a Ca^{2+} dependent switch for crossbridges to a form available to bind actin. The mathematical formulation of the crossbridge cycle rates used here are adopted from [2].

The model of thin filament includes a continuous flexible chain (CFC) representation [32, 33] for tropomyosin and structural changes such as variation of sarcomere length, interfilament sarcomere lattice spacing and length dependent effects of titin forces. These features enabled simulations that showed excellent predictions of the magnitude and kinetics of twitch tension in response to physiological Ca^{2+} transients in cardiac muscle [2].

2.2. New features for modeling twitch contractions in transgenic mice trabecula

We do not have a set of experimental Ca^{2+} transients for the transgenic mice and it is important to note that the Ca^{2+} transients cannot be assumed to be the same as for WT cardiac muscle with mutations that alter Ca^{2+} binding properties of cTnC. TnC is the largest Ca^{2+} buffer in myocytes and alterations in TnC Ca^{2+} affinity may alter Ca^{2+} homeostasis in myocytes. Davis et al. made a careful study of the Ca^{2+} transients for the three transgenic mice used here and we used these Ca^{2+} transients as a guide [1]. The method for estimating these Ca^{2+} transients is described in the Supplemental Material (Fig. S2).

For modeling the twitch transients in L48Q and I61Q transgenic mice it is necessary to include structural details and the distribution of the mutant cTnCs amongst WT cTnCs in thin filaments, a novel feature that allows simulations of mutational incorporation (see Fig. 1C). The explicit sarcomere structure in our model also allowed the implementation of mixtures of WT and mutated cTnCs, distributed either randomly or in clusters of 2–3 mutated cTnCs along each strand of Tm chain within individual thin filaments. Keeping the same proportion of WT vs. mutated TnCs as simulated for the transgenic mice, we quantitatively estimated the effect of different distributions on the amount of developed active tensions.

2.3. Twitch experiments in intact trabeculae

Thin, unbranched, and intact trabeculae were carefully dissected from the right ventricular wall of wild-type and transgenic mice and mounted between a force transducer (Cambridge Technology, Inc., Model 400A) and a length-controlling motor (Aurora Scientific, Model 300C). Each end of the trabecula was sutured to custom arms attached to the motor and force transducer made from 22-gauge needles. The trabecula was then submerged in a custom-built experimental chamber that was continuously perfused with modified Krebs buffer, containing (in mM) 118.5 NaCl, 5 KCl, 1.2 MgSO4, 2 NaH2PO4, 25 NaHCO3, 1.8 CaCl2, and 10 glucose, at 30° C. Twitches were elicited by field stimulation with custom platinum plate electrodes at 1 Hz with oscillating polarity and intensity 50% above threshold. Sarcomere length (SL) was set to 2.0 μm using an inverted stereomicroscope with a 40x dry objective lens and a 10x eyepiece. If sarcomeres could not be seen (e.g., if the trabecula was too thick), a SL of 2.0 μm was assumed to be at trabecula slack length (the length of the trabecula at the onset of passive tension development). Trabeculae were allowed to pace at 1 Hz for ~20 minutes at SL 2.0 μm (and 30°C), and then stretched to SL 2.3 μm for data acquisition. Continuous twitch force traces were recorded using custom

LabView software at a sampling rate of 1 kHz and were analyzed with custom code written using MATLAB software (The MathWorks, Natick MA).

2.4. Model parameters and simulations performance.

A complete set of model parameters used in simulations of WT mouse trabecula twitch experiments at 30 °C are displayed in Table 1. For clarity, we discuss below the origin and definitions of several parameters adjusted in simulations of the experiments performed on transgenic mouse trabeculae including mutations (Table 3) or parameters contrasting the differences between species, e.g., mouse vs rat (Table 2).

All simulations, paralleling the experiments, were performed at temperature of 30° C, and at sarcomere lengths 2.3 μm in mice and 2.2 μm in rats. Actin filaments can vary in length, depending on species, typically in the range of 0.6 to 1.1μm (e.g., in rat atrial trabecula [34]) and they have a monomer spacing of ~2.735 nm and the half period of one strand is 35.56 nm under relaxed conditions [35–37]. The length of a myosin filament is ~1.58 μm, having 50 crowns, i.e. 150 myosin molecules per half-thick filament, with a crown spacing of 14.3 nm [38]. The values of the interfilament spacing $d1,0$ are specified for each set of simulations [39]: in intact mouse trabecula $d1,0$ ~33.10 nm at SL 2.3 μm and in rat trabecula ~33.83 nm at SL 2.2 μm. The inter-filament spacing is an important factor in modulation of myosin binding to actin and, possibly other rates in crossbridge cycle [29, 40].

Actin and myosin filaments are extensible with filament moduli (elastic modulus times cross-section area) derived from X-ray diffraction or direct measurement: for actin, $K_a = A_aE_a$ and for myosin $K_m = A_mE_m$ taken from [35, 41] and shown in Table 1. We used here the modulus, AE, rather than stiffness, AE/L, because the reported stiffness values depend on the filament length, L, and cross-section area A is not well defined for myosin and actin filaments. The nonlinear elasticity of titin is adopted from [29] and used in all simulations. Moreover, following the approach of Mijailovich et al. [2], the series elasticity of trabeculae is derived from the experiments of Caremani et al. [42] and used in all simulations.

For Ca^{2+} binding kinetics to TnC and interaction of TnI with actin (Fig. S1), the equilibrium rate constant of Ca^{2+} binding to TnC, $\tilde{K}_{Ca}$, along TnC closed states, is effectively defined via the forward constant $k_{Ca} = \tilde{k}_{Ca} \cdot [Ca]$ (for the definitions see [2]). The parameters defining rates $\tilde{k}_{Ca}$, k_{-Ca}, TnI-actin interaction equilibrium rate, λ, and constant cooperativity coefficient, ε_0, for WT mouse are shown in Table 1. The values of parameters different than those in Table 1, specific for mouse mutant myocardium are shown in Table 3. For the CFC model parameters we used those reported in [2].

Due to the stochastic process of myosin interacting with actin, the forces in the myofilaments fluctuate in time and each filament experiences somewhat different force. For comparison with observed isometric tensions we include in all plots both the tension in kPa and the average force per myosin filament, F, in pN. The scales are related by a factor that takes into account how many myosin filaments there are per unit fiber cross-sectional area [28, 43]. Because the total number of thick filaments in a myofibril or muscle fiber does not change with experimental conditions, for the estimation of the number of thick filaments per

unit of cross section area, we used the lattice spacing, d1,0, at the same length where the muscle cross-sectional area is measured for calculations of the muscle tension.

In intact trabeculae, the lattice spacing at a sarcomere length of 2.0 μm, where the cross-sectional area was measured, is d1,0=35.49 nm [39] and the number of thick filaments per μm2 myofibril is ~688. Considering that the fraction of the cross-sectional area in rat trabeculae occupied by myofibrils is ~ 61 % [44, 45], this reduces the number of myosin filaments over the trabeculae cross-section to ~420 per μm2. In this case, the scaling factor provides that T_o =50 kPa corresponds to F_o=119.2 pN per myosin filament or 59.6 pN per actin filament.

2.5. Modelling the Mouse wild-type twitch

Using the MUSICO platform we previously demonstrated simulations of twitch tension transients that closely matched those observed for rat trabeculae under a variety of conditions [2]. The model used a set of intrinsic parameters based on experimental measurements from multiple research groups (see Tables 1 and 2) [9, 42, 46]. The key difference between the twitch in the mouse versus rat muscle is the time course of the tension development and relaxation, with these being more rapid for mouse cardiac muscle, for example twitch time parameters are 1.5 to 2 times shorter in mouse [47] than in rat [48]. This, primarily due to differences in myosin kinetics, is a general phenomenon amongst muscle myosin isoforms where the equivalent isoform is faster the smaller the mammal ([49], see Discussion). For example, motility assays and ATPase rates are 2–3 fold faster in mouse cardiac myosin (exclusively the α-myosin isoform) than in rat cardiac myosin (which expresses 90% α and 10% β-myosin isoform [50, 51]) in addition to myofibril activation and relaxation kinetics being faster for mouse cardiac muscle [9] than for rat [52]. The changes made in the rat model parameters to model mouse data are described in Table 2. The rate constants for myosin binding and detachment from actin, ATP hydrolysis and ADP release (highlighted in Table 2) were increased by a factor of 1.5 to 3, compatible with experimental studies of rat and mouse contraction parameters in skinned cardiac muscle, myofibrils and myosin [9, 50–56]. The exceptions to the 1.5 to 3 increase are the rate constants of the power stroke (k_{+Pi} and k_{-Pi}) which were increased by a factor of 10 for the mouse (displayed in Table 2 via k_{+Pi}^{cap}), such that the equilibrium rate K_{pi} is unchanged. Note that the Pi release step controlled by constant K_{Pi} is assumed to be in rapid equilibrium, and k_{+Pi}^{cap} =1000 s^{-1} was adequate for rat simulations, but k_{+Pi} and k_{-Pi} had to be increased for the mouse by 10-fold, thus we used $k_{+Pi}^{cap} = 10000 s^{-1}$.

Figure 2 shows the time course of a twitch in mouse trabeculae at 30° C with a sarcomere length of 2.3 μm (*solid line*), averaged from the data for wild type (WT) mice. In these experiments, Ca^{2+} transients were not measured for WT type mice or for their transgenic littermates that express cTnC mutations. Instead, the Ca^{2+} transients used in simulations were derived from Davis et al. [1], which reported on these same transgenic mouse lines (for the derivation details see Supplemental Material, Fig. S2). Model simulations matched the tension amplitude and time course of the twitch quite well (*dashed line*, Fig. 2A). This was in part due to accounting for the internal (half) sarcomere length shortening (*dashed line*,

Fig. 2B) that occurs in trabeculae where the total trabeculae length is held constant during twitch contractions [42, 57]. Because the values for Ca^{2+} transients from Fig. S2 were estimated, the effect of ± 20% change of the [Ca^{2+}] transient is quantified for the twitch tension transients for WT and $cTnC^{I61Q}$ (see Fig. S3). The parameters used in simulations are the same as used in simulations shown in Fig. 3. Furthermore, the details related to the effect of change in sarcomere length on the twitch tension are shown in Fig. S4. These simulations of trabeculae from WT transgenic mice provided initial validation for the parameter values that were adjusted from rats to mice.

3. Results

Twitch contractions were collected for intact trabeculae from the WT and transgenic mice expressing 30% (cTnCL48Q) or 50% of ($cTnC^{I61Q}$) of the mutant cTnC as described in the Methods. The experimental data is summarized in Fig. 3, shown as an average of N observations, specified for each case in the legend of Fig. 3. The twitch peak tension (Fig. 3A) and time parameters that characterize tension rise (Figs. 3 B and C) did not differ between trabeculae from WT versus L48Q mice. In comparison, peak tension was reduced by ~60 % for trabeculae from I61Q versus WT mice (Fig. 3A), but rates of force development (Figs. 3 B and C) did not differ. Relaxation times were significantly lengthened for L48Q muscles (Figs. 3 D and E) but unchanged for I61Q muscles. This slower relaxation for cTnCL48Q reflects a three-fold increase in the affinity of Ca^{2+} for cTnC due to a slower Ca^{2+} dissociation (k_{-Ca}) rate constant (cTnCWT = 75 ± 5 s^{-1}; cTnCL48Q = 28 ± 4 s^{-1}), as previously reported [9, 17–19]. In contrast, $cTnC^{I61Q}$ has a three-fold weaker affinity for Ca^{2+} due to a faster Ca^{2+} dissociation rate constant (237 ± 30 s^{-1}) [9, 17–19]. This resulted in the much lower peak tension (due to a lower Ca^{2+} activation level), even though the time course of the tension transient was not significantly affected.

Fig. 3F compares experimental twitches (*solid lines*) to twitch simulations using our MUSICO platform (*dashed lines*) driven by the Ca^{2+} transients (*dotted lines*) measured in Davis et al. [1], and model estimates of sarcomere length changes occurring during the twitch. The simulated twitches match the peak tension, the tension development and relaxation kinetics of the experimental data in each case. Table 3 lists the small number of parameters that were needed to be adjusted to fit the three transients. Fitting our six-state cross bridge cycle model to the tension data for both transgenic mouse lines was achieved primarily by changing the rate for Ca^{2+} dissociation from cTnC (k_{-Ca}) for the proportion of cTnC mutant found in mouse trabeculae sarcomeres (Table 3). The k_{-Ca} was changed by similar magnitudes to that we have reported from experimental measurements, e.g., a three-fold increase compared to WT for $cTnC^{I61Q}$ and a three-fold decrease for cTnCL48Q [9, 17, 18]. Protein biochemical measurements, previously reported, indicate this resulted in a similar fold increase in cTnCL48Q affinity for cTnI [17] and a similar fold decrease for $cTnC^{I61Q}$ [18]. The cTnCs containing mutations were assumed to be randomly distributed in thin filaments throughout the sarcomere (Fig. 1C). Alternate distributions are considered in section 3.2. These simulations gave a reasonably good fit to the data during tension rise, but not during relaxation (Fig. 4). To generate the best fits shown in Fig. 3F required adjustment of two additional parameters, specifically the rate constant (k^{o}_{-A}) for actin dissociation from

the A-M.D.Pi complex and the equilibrium constant (λ) for the interaction between cTnI and actin (see Table 3). The arguments for why these changes are reasonable are considered below.

3.1. Mutation Incorporation into Myofilaments

One issue that has been difficult to address in previous modelling studies is the ability to simulate less than 100% of a mutant isoform in cardiomyocytes. An advantage of structure-based sarcomere models like MUSICO is the ability to define the properties of each cTnC along a thin filament and between thin filaments, thus allowing varying the ratios of and position of cTnC containing mutations in simulations, something that cannot be accomplished experimentally in transgenic mice. For the transgenic mice in these studies, the myofibril incorporation level of $cTnC^{L48Q}$ was 30% while that of $cTnC^{I61Q}$ was 50%. In initial simulations (Fig. 3F) we accounted for this incorporation by assuming a random distribution of the mutation in each thin filament to achieve the 30% (TnCL48Q) and 50% ($cTnC^{I61Q}$) levels measured in cardiac muscle of the transgenic mice.

In Fig. 5 the predicted effect of varying mutation incorporation is explored for the two mutations. Fig. 5A demonstrates variation in $cTnC^{I61Q}$ incorporation from 0 to 100%, predicting a decrease in peak tension as the percentage of $cTnC^{I61Q}$ increases, assuming the Ca^{2+} transient remains the same. Peak force decreased from ~120 pN/myofilament with cTnCWT to ~12 pN/myofilament with 100% $cTnC^{I61Q}$. The reduction of peak tension relative to increasing $cTnC^{I61Q}$ is quantitatively expressed in Fig. 5C and demonstrates that peak twitch force is more sensitive to $cTnC^{I61Q}$ at lower incorporation compared to high. In contrast, as the % of $cTnC^{L48Q}$ present in myofilaments increases there is a linear increase in peak force from ~105 to 140 pN/myofilament (Fig. 5 B and C). In both cases the time to peak tension was little affected, while the 50% relaxation time (RT50) mirrors the behavior of the peak tension i.e., it is significantly shorter for $cTnC^{I61Q}$ but increases marginally for $cTnC^{L48Q}$. The observations suggest that low levels of $cTnC^{I61Q}$ should have a larger effect than cTnC L48Q on the contractile properties of myocytes. By implication, this suggests that the contractile properties of cardiomyocytes are more affected by increasing the Ca^{2+} dissociation rate of cTnC as observed in $cTnC^{I61Q}$ than decreasing it as in $cTnC^{L48Q}$.

3.2. Mutation Clustering

The thin filament is a highly cooperative system and the distribution of cTnC mutations could induce positive or negative cooperativity between adjacent cTnC's within a thin filament. In addition, there is evidence that cTnC can be exchanged more readily in different parts of the sarcomere [58, 59]. An advantage of structure-based sarcomere models is the ability to study the influence of mutation clustering along the length of thin filaments or differential incorporation between thin filaments or between different regions of a thin filament in myocytes. As mentioned above, this manipulation is not possible in animal models. An analysis of mutant cTnC clustering is presented in Fig. 6. For these analyses, the level of incorporation for each mutation was assumed to be the same as what was present in the transgenic mice and used in simulations with random distribution of mutant and WT cTnCs (Fig. 3). We considered the effect of mutant cTnCs binding cooperatively on the thin filament causing increased clustering as illustrated in Fig. 6A. Interestingly, the effect of this

clustering on tension transients for either mutation was minimal (Fig. 6B). An extreme example of cTnC clustering would be the case where cTnC mutations segregate into separate thin filaments, with some filaments not containing any mutant cTnCs and others containing only the mutant cTnC (Fig. 7). In this case only 30% of thin filaments contained 100% $cTnC^{L48Q}$ and only 50% filaments contained 100% cTnC I61Q. As shown in Fig. 7, the effect of this extreme segregation was minimal for $cTnC^{L48Q}$ while simulations for the $cTnC^{I61Q}$ mutation predicts ~50% higher peak tension than for the random distribution of $cTnC^{I61Q}$s along each thin filament.

3.3. The effect of mutations on rates of cTnI dissociation from cTnC-cTnI and dissociation of myosin from A.M.D.Pi state

As mentioned above, in addition to the Ca^{2+} dissociation rate constant, k_{-Ca}, two other parameters had to be changed to generate the best fits shown in Fig. 3F. These were the myosin-actin dissociation rate k^{o}_{-A} and the equilibrium constant between A + TnI-TnC.Ca^{2+} $\rightleftarrows$ A-TnI + TnC.Ca^{2+}, denoted as λ in Fig. S1.

During relaxation sarcomere length increases and a significant number of crossbridges in the A.M.D.Pi state are trapped maintaining high tension. Furthermore, the number of these crossbridges is even increased further due to reverse power strokes associated with sarcomere lengthening. Because these crossbridges cannot complete full crossbridge cycle their detachment can only be realized via k^{o}_{-A} pathway, and, in most of the cases, the dissociation rate k^{o}_{-A} needs to be adjusted to match the observed tensions and sarcomere length changes. The effect of keeping k^{o}_{-A} constant at the WT value is simulated in Fig. 4A (*dotted lines*). In both mutant cases WT value of k^{o}_{-A} resulted in a faster relaxation than observed but after adjusting the value of k^{o}_{-A} to match the experimental data, k^{o}_{-A} was reduced by ~30% for L48Q trabeculae (from 115 for WT to 80 s^{-1}) and decreased even more (~ 50 %) for I61Q trabeculae (i.e., to 60 s^{-1}). The smaller values of k^{o}_{-A} resulted in a slower relaxation (dashed lines) but had little effect on the rise time or peak tension. A similar effect to reducing k^{o}_{-A} could be achieved by slowing both maximum forward and backward rates of the parked state while keeping $k^{\max}_{PS}/k_{-PS}$ fixed at a value of ~2, while keeping WT k^{o}_{-A} values (Fig, 4B). In this case, the PS state reduces the population of M.D.Pi state at decreased [Ca^{2+}] levels causing a significant reduction in binding flux and, therefore, having the same effect as reduction in k^{o}_{-A}.

For the best fits shown in Fig. 3F, the value of λ, the equilibrium constant between A + TnI-TnC $\rightleftarrows$ A-TnI + TnC, was increased by a factor of 2 (from 10 to 20) for $cTnC^{L48Q}$, and reduced by a factor of ~7 for $cTnC^{I61Q}$. Note that these changes are in the opposite direction for the two cTnC mutations. A change in the interaction between cTnI and cTnC for the two cTnC mutations that alter Ca^{2+} binding affinity is likely to induce an altered balance of cTnI's affinity for actin versus cTnC (λ). Note, we do not suggest that the affinity of TnI for actin has changed just the balance of the competition between the two ligands for TnI. Fig. 4C shows the effect of keeping λ constant at 10, i.e., the value for WT. The effect is minimal

for cTnC^{L48Q}, while for cTnC^{I61Q} the change causes a greater than two-fold increase in peak tension with little change in time to peak tension or relaxation rate. A low value for λ means that Ca^{2+} bound to cTnC does not compete well with actin for binding cTnI and so is less effective at switching on thin filaments. This is consistent with demembranated rat cardiac muscle data [9] where completely exchanged cTnC^{I61Q} into rat cardiac myofibrils could generate only 40% of the tension of WT myofibrils, even at saturating [Ca^{2+}].

4. Discussion

The effect of mutations in sarcomere proteins on the function of the contractile apparatus is complex for diseases such as hypertrophic and dilated cardiomyopathy. In addition to altering the properties of the individual protein, mutations differ in terms of their effects on disease progression and severity. These differences likely result from multiple factors, including mutation incorporation, position of the protein in the contractile apparatus and haplo-insufficiency. There is experimental evidence to suggest that small fractions of a particular mutation in sarcomeres can have a significant or even dominant effect on the contractile properties of cardiomyocytes [20, 60]. To determine how mutation incorporation and location within sarcomeres influence contractile function is difficult to address experimentally, but this can be studied quantitatively with spatially explicit, stochastic-kinetic cardiomyocyte models. The MUSICO model platform provides features that allow individual proteins to have independent kinetic signatures. The platform is able to fit both the WT and mutant mouse twitch tension transients using the same model, and the same set of base parameters as used for the rat trabeculae (Table 2). Thus, the current study provides validation of this modelling approach and its usefulness to examine muscle cell properties across multiple species with different sarcomere protein isoforms. It can predict the magnitude and time course of twitch tension for cardiac muscle, and how this is affected by varying levels of mutant proteins. It is, therefore, a useful tool to evaluate whether mutation clustering within or between filaments differentially affects the twitch magnitude or time course of contraction and relaxation.

In this study, we examined two mutant cTnCs with increased (cTnC^{I61Q}) or decreased (cTnC^{L48Q}) rate constants of Ca^{2+} dissociation, to further validate the model and begin to examine the roles of mutation incorporation and position within sarcomeres. We found that changing the Ca^{2+} dissociation rate was sufficient to simulate the rising phase of the twitch from transgenic mice containing a known incorporation of each mutation, but was not as effective at fitting the time course of relaxation. For relaxation, the best-fits were achieved by also adjusting the equilibrium rate of TnI interaction with actin (λ) when Ca^{2+} is bound to cTnC, and the rate of myosin detachment from actin (k^{o}_{-A}) (see below). The changes made in Ca^{2+} dissociation rate constants for the simulations were the same as those measured experimentally *in vitro* [9, 19, 61]. The magnitude of the twitch was more sensitive to faster Ca^{2+} dissociation kinetics compared with slower kinetics. On the other hand, relaxation kinetics were sensitive to slower Ca^{2+} dissociation kinetics (cTnC^{L48Q}) but little affected by faster Ca^{2+} dissociation kinetics (cTnC^{I61Q}).

cTnC^{I61Q}

Trabeculae from mice expressing 50% cTnC^{WT} and 50% cTnC^{I61Q} showed much lower peak tension than trabeculae from WT mice (Fig. 3A), but a similar time course for both the rise and fall of the tension transient. Myofibril data from Kreutziger et al. [9], where native cTnC in myofibrils was replaced almost completely with cTnC^{I61Q} also shows relaxation not being affected but the activation kinetics in myofibrils had normalized k_{ACT} and k_{TR} traces that were as fast as from WT. However, at pCa = 4.5 I61Q myofibrils show lower steady state tension than in WT, and a slower rate of tension rise, that is consistent with lower peak tension and slower tension rise during twitch of intact I61Q trabecula considering the 50% incorporation of cTnC^{I61Q}. This can be almost entirely accounted for the lower affinity of TnC for Ca^{2+} and more than compensates for the higher peak [Ca^{2+}] predicted during the cardiac twitch. The ~3 fold faster rate of Ca^{2+} dissociation from cTnC did not accelerate the observed rate of relaxation even though the predicted Ca^{2+} transient also returned to the basal level more quickly than for WT simulations, both of which might have been expected to accelerate relaxation. This issue is easier to understand using the incorporation data of Fig. 5 where the same Ca^{2+} transient is used at each level of cTnC^{I61Q} incorporation into thin filaments. These simulations predict that peak tension should decrease as the fractional saturation of thin filaments with cTnC^{I61Q} increases (Fig. 5), due to the increased fraction of total cTnC with lower affinity for Ca^{2+}. The time course of the tension transient was less affected than the magnitude. The time to peak was only marginally shorter as cTnC^{I61Q} was increased from 0% to 100% though the time to 50% peak tension was longer by ~ 20% for 100 % cTnC^{I61Q}, due mainly to an increase in the lag at the start of tension rise. The relaxation kinetics was affected more. They were not significantly affected until TnCI61Q was half of total cTnC in thin filaments, but both 50% and 90% relaxation times were almost twice as fast as with 100% cTnC^{I61Q}. This result is consistent with the idea that faster release of Ca^{2+} from cTn results in faster deactivation of the thin filament. In a previous myofibril study mentioned above [9], where native cTnC in isolated sub-cellular contractile organelles (myofibrils) was totally replaced by cTnC^{I61Q}, the maximum steady state tension of individual mouse cardiac myofibrils at saturating Ca^{2+} was reduced by 50% but the rate of relaxation was not affected. The apparent difference in these results may be explained by the high level of Ca^{2+} in the activation solution (300 μM), which is approximately two orders of magnitude greater than that seen in the Ca^{2+} transient that precipitates the cardiac twitch. At the much lower, and transient Ca^{2+} levels of the twitch, other factors may be influencing the rate of relaxation, including a lower threshold for the removal of [Ca^{2+}] before relaxation is initiated and the smaller number of force-bearing crossbridges at peak tension. Martyn and Fuchs have demonstrated that crossbridge binding has a positive, cooperative effect on Ca^{2+} binding to cTn in cardiac muscle [62–64]. Thus, fewer crossbridges likely results in reduced thin filament activation that may allow acceleration of deactivation during relaxation as intracellular Ca^{2+} is sequestered.

cTnC^{L48Q}

Trabeculae from mice expressing 30% cTnC^{L48Q} (and 70% cTnC^{WT}) had a similar rate of tension rise and peak tension as trabeculae from WT littermates, but the rate of relaxation was significantly slower. The model suggests that the slower rate constant of Ca^{2+} dissociation from cTnC^{L48Q}, k_{-Ca}, can account for the slowed relaxation. This observation is

consistent with the results of Kreutziger et al. [9] on isolated myofibrils, with almost complete exchange of native TnC by cTnC^{L48Q}, where the slow relaxation phase duration was increased and fast phase relaxation rate was slower with little effect on maximum steady state tension. The longer slow phase duration was attributed to the thin filament staying turned on longer due to slower k_{-Ca} of troponin with cTnC^{L48Q}. This suggests that slowing Ca^{2+} release from thin filament cTn can significantly impair the rate of relaxation. In the twitches of trabeculae from transgenic mice, the ~ 3-fold higher affinity of cTnC^{L48Q} for Ca^{2+} did not lead to a higher level of peak tension. This is likely because the peak [Ca^{2+}] transient for the cTnC^{L48Q} trabeculae was 20% lower that for cTnC^{WT}. These two opposing factors likely cancel each other out, resulting in a similar level of activation.

The simulations presented in Fig. 5 predict that, as the incorporation of cTnC^{L48Q} increases from 0 to 100% (assuming a fixed Ca^{2+} transient), the peak force should increase linearly by ~3% (~3.5 pN/myofilament) for each 10% increase in cTnC^{L48Q} incorporated into thin filaments. Under these conditions, the system is not saturated with Ca^{2+} and peak force is proportional to the fraction of cTnC^{L48Q} that is present. The rate of relaxation slows marginally (RT50 increasing from 80 to 100 ms) suggesting only a modest effect of the three-fold slower Ca^{2+} release rate constant on relaxation. This is consistent with the mouse myofibril data where total replacement of native cTnC with cTnC^{L48Q} resulted in the duration of the slow relaxation phase increasing from 59 ± 4 ms to 85 ± 6 ms while the fast phase of relaxation slowed from 21.8 ± 3 s^{-1} to 14.5 ± 1.4 s^{-1} [9].

The dose dependence of cTnT mutant incorporation on Ca^{2+} showed the same trend as for the cTnC, where several mutants increased the Ca^{2+} sensitivity (I79N and R94C) and the other decreased sensitivity at high doses of mutant (R278C) [6]. However, at low doses of cTnT^{R278C} the sensitivity showed the opposite trend. This difference can be attributed to the location of mutations, which is considered in this study on cTnC and in Schuldt et al. [6] on cTnT. These mutations affect the thin filament regulation by two distinctive mechanisms: cTnC mutations directly affect thin filament regulation by Ca^{2+} via changing affinity of TnI for actin after Ca^{2+} binds to or dissociates from cTnC and therefore the Ca^{2+} sensitivity, whereas in the Schuldt et al. case, cTnT affects the interaction between neighboring tropomyosins, i.e. cTnT modulates elasticity of continuous flexible chain (CFC), thus the thin filament regulation is affected by altered CFC lateral mobility [33], not by changes in Ca^{2+} affinity to TnC. Therefore, the sensitivity analysis of mutilations of cTnC analysis cannot be directly translated to the changes in Ca^{2+} sensitivity caused by cTnT mutations.

Why does λ change?

The change in λ (two-fold larger than WT) has only a minor effect on the time course of the transient for cTnC^{L48Q} simulations. For cTnC^{I61Q}, λ is seven-fold smaller than WT and is required to reduce the peak tension to fit the observed tension. The definition of λ is the equilibrium constant between TnI bound to actin or TnI bound to TnC (A + TnI-TnC $\rightleftarrows$ A-TnI + TnC). A mutation in cTnC that alters its affinity for Ca^{2+} is also likely to alter the affinity of cTnC for cTnI (more precisely the cTnI switch peptide) and alter the balance between cTnI affinity for actin and cTnC. Data from rat myofibrils suggests that cTnC^{I61Q} myofibrils cannot be fully activated even at saturating [Ca^{2+}] [9]. This is consistent with a

reduced affinity of cTnC^{I61Q} for cTnI leading to incomplete activation. This is also consistent with the notion that that mutation does not simply affect Ca^{2+} affinity and the rate of Ca^{2+} release, but also significantly reduces the value of λ.

Why does k_{-A} or k_{PS} change in the presence of the TnC mutations?

Our simulations show that just changing the WT values for the rate of Ca^{2+} release from cTnC and λ gives a reasonable fit to the peak tension and the rising phase of tension rise. The relaxation phase is not well described without additional parameter changes. The relaxation phase is the most difficult part of the twitch transient to fit. Multiple factors contribute to this process including cooperativity in the relaxation of the thick and thin filaments, the rates of Ca^{2+} release and the net detachment rates of crossbridges. These can involve the rate of ADP release from the bound myosin head, ATP binding to the myosin head, and the reversal of the power-stroke to a weakly attached state. In addition, during the relaxation phase, sarcomeres are lengthening putting additional strain on attached crossbridges, which can accelerate detachment of weakly bound crossbridges and slow down the release of ADP from strongly bound A.M.D crossbridges. In our simulations of the mutant myocardium, when we only change the rate of Ca^{2+} release and λ, we can fit the peak tension and rate of tension rise well but the relaxation phase is too fast. As shown in Figs. 4A and B this can be corrected by either a change in (k^o_{-A}) or adjusting the rate of entering and leaving the parked state (Adj. k_{PS} and k_{-PS}, Fig. 4B) but leaving the equilibrium constant, K_{PS}, unchanged. The same effect can be produced by a combination of k^o_{-A} and k_{PS}. We chose to use change in k^o_{-A} since these were modest (reduced by ~30% for L48Q or by ~50% for I61Q) compared the much larger reduction required for the PS rate constants (4-fold for L48Q or almost 8-fold for I61Q).

There is no obvious way in which a mutation in cTnC would be expected to exert a direct effect on either k^o_{-A} or k_{PS}, which suggests that these parameters could be complex terms reflecting more than one underlying process. Altering kinetic parameters of Ca^{2+} binding to and dissociation from with cTnC and changes in affinity of cTnI to actin in order to match the observations without changing crossbridge rates would require strong experimental evidence justifying such changes. Part of the problem could be in uncertainties in Ca^{2+} transients that were estimated form Davis et al. [1] experiments, using the observed Ca^{2+} transient decay time in isolated adult rat cardiac myocytes not in intact mouse trabeculae. Fine tuning of Ca^{2+} decay tails in order to match the observed tension transients is complex and speculative. In addition, the absence of a known mechanism connecting mutations in cTnC with state transition rates in crossbridge cycle, the chosen changes in detachment rate k^o_{-A} or alternatively the parked state rate constants ($k^{\max}_{PS}$ and k_{-PS}) are rather a convenience for achieving good fits than representing a well-defined underlying mechanism. While this is likely to be true for both terms, a common feature of both k^o_{-A} and k_{PS}, is that they control the net rate of entry into the PS (= [M.D.Pi] k_{PS} – [PS] k_{-PS} where M.D.Pi is in equilibrium with A-M.D.Pi) and are both controlled by the relatively rapid equilibrium constant. K_A A change in the availability of actin sites during the relaxation phase due to the mutation in cTnC, which is not adequately captured by our model, could be accounted for by a change in

k^{o}_{-A}. This is most likely to be due to the complexity of the cooperativity of the relaxation process across both thick and thin filaments.

The PS is defined in simple terms in our model, as it remains under-defined experimentally. The fraction of myosin head in the PS under different conditions is not well known and there may be multiple forms, e.g., both heads tightly constrained to the thick filament, both heads released from the thick filament but still interacting with each other, or both heads free to interact with actin. Additionally, the thick filament is not uniform, and the role of cMyBP-C remains to be fully defined. cMyBP-C may be involved in stabilizing the PS and potentially in maintaining the thin filament in an activated form. One challenge in understanding the role of cMyBP-C is that it is only present in the C-zone of the thick filament and in this region it is present in only 1 in 3 myosin crowns. There is a potential for cTnC mutations to influence the interaction of MyBP-C with actin and hence slow relaxation.

Our model assumes a rapid, Ca^{2+}-dependent, equilibrium between the M.ADP.Pi state and the PS, to allow PS activation to follow Ca^{2+} dependent thin filament activation. For our simulations, we made no change to the Ca^{2+} binding properties of the PS since there is no expectation that the cTnC mutations would directly alter thick filament properties. Note, however, that in the model, the transition into the PS is assumed to be rapid (200 s^{-1}) and therefore unlikely to affect the rate of relaxation. There is one aspect of the PS that becomes apparent from examining the $cTnC^{L48Q}$ data. The high Ca^{2+} affinity of $cTnC^{L48Q}$ means that at 100 % $cTnC^{L48Q}$ even at resting Ca^{2+} levels (~0.1 μM) the thin filament is ~25% saturated with Ca^{2+} and therefore in the absence of a PS a significant level of “active resting tension” is predicted [24]. This is not observed because the PS keeps the system turned off. This is demonstrated in simulations of force-pCa relations observed in myofibrils [24].

Clustering

One of the major advantages of the explicit 3-D modelling in the MUSICO platform is the ability to model both variable incorporation of a mutation and variation in the localization of the mutations, separately or in combination. Surprisingly, our simulations suggest that clustering of mutant cTnC within individual thin filaments appears to have little effect on the cardiac muscle twitch (Fig. 6B). The effect of incorporation of increasing amount of $cTnC^{I61Q}$ demonstrated modest cooperativity in the downward curvature of the peak tension plot (Fig. 6C). If the mutated cTnC are segregated in separate actin filaments than $cTnC^{WT}$, then the effect of this cooperativity is negated, and predicted peak tension shows a linear decrease in response to increase of $cTnC^{I61Q}$ dose. Even when total segregation of the mutations was explored i.e., when mutations were confined to individual filaments, the effects were minor for $cTnC^{L48Q}$ and significant $cTnC^{I61Q}$ (*dotted lines* in Fig. 7). Because the effect of incorporation of the mutations in segregated filaments shows no cooperativity then, therefore, the location of TnC within the sarcomere had no influence on the peak tension.

Tension-Time Integral and Model Implications

Recent studies [1, 21] have demonstrated that the tension-time integral of a twitch from cardiac muscle carrying sarcomere mutations is highly correlative with the type and severity

of myocardial growth and remodeling. Termed the 'tension index (*TI*),' this metric accurately distinguished HCM and DCM remodeling of cardiomyocytes from animal models and cardiomyocytes differentiated from human inducible pluripotent stem cells. We recently demonstrated that the predictive capacity of *TI* extends to the whole heart level and to targeted genetic engineering to prevent phenotypic development [21]. These models open the possibility of investigating the sensitivity of the *TI* on a multitude of DCM- or HCM-causing sarcomere mutation and their incorporation in the myofilaments. The *TIs* for the $cTnC^{L48Q}$ and $cTnC^{I61Q}$ mutations from 0–100% incorporation were calculated (Fig. S5), and revealed that the *TI* is more sensitive to $cTnC^{I61Q}$ at low incorporation compared to $cTnC^{L48Q}$, suggesting a high degree of cardiac remodeling for this variant even at low expression levels.

The present study demonstrates the value and versatility of spatially explicit models of the sarcomere and represents a new platform for predicting the malignancy of sarcomere protein mutations that affect twitch tension. It also has the capacity to study how distribution of mutations within myofilaments may impact the functional phenotype, as the models allow for individualize properties of each protein within the framework of sarcomere structure. The work presented here is limited to TnC mutations that alter the Ca^{2+} affinity of troponin. Future work will explore the ability of our approach to model different types of mutations in troponin and other sarcomere proteins. In addition to mutations, these models can be applied to study mixed populations of protein isoforms, such as cardiac β- and α-myosin, or the effects of variable post-translational modifications such as phosphorylation. Finally, in combination with calculations of *TI*, they can be used to predict the effect of tension-targeted therapeutic strategies being developed.

Supplementary Material

Refer to Web version on PubMed Central for supplementary material.

ACKNOWLEDGEMENTS

This project is supported by grants NIH R01 HL128368 (M.R.), RM1 GM131981 (M.R.), P30AR074990 (M.R.) and the European Union's Horizon 2020 research and innovation programme under grant agreement No 777204 (S.M.M., M.R., M.A.G., C.P.). We are also gratefully acknowledging the help of Prof. Thomas C. Irving with editing the final version of the manuscript.

References

[1]. Davis J, Davis LC, Correll RN, Makarewich CA, Schwanekamp JA, Moussavi-Harami F, Wang D, York AJ, Wu H, Houser SR, Seidman CE, Seidman JG, Regnier M, Metzger JM, Wu JC, Molkentin JD, A Tension-Based Model Distinguishes Hypertrophic versus Dilated Cardiomyopathy, Cell 165(5) (2016) 1147–1159. [PubMed: 27114035]

[2]. Mijailovich SM, Prodanovic M, Poggesi C, Geeves MA, Regnier M, Multiscale Modeling of Twitch Contractions in Cardiac Trabeculae, Journal of General Physiology 153 (3) (2021) e202012604.

[3]. Gordon AM, Homsher E, Regnier M, Regulation of contraction in striated muscle, Physiol. Rev. 80(2) (2000) 853–924. [PubMed: 10747208]

[4]. Tardiff JC, Thin filament mutations: developing an integrative approach to a complex disorder, Circ Res 108(6) (2011) 765–82. [PubMed: 21415410]

[5]. Regnier M, Rivera AJ, Wang CK, Bates MA, Chase PB, Gordon AM, Thin filament near-neighbour regulatory unit interactions affect rabbit skeletal muscle steady-state force-Ca(2+) relations, J Physiol 540(Pt 2) (2002) 485–97. [PubMed: 11956338]

[6]. Schuldt M, Johnston JR, He H, Huurman R, Pei J, Harakalova M, Poggesi C, Michels M, Kuster DWD, Pinto JR, van der Velden J, Mutation location of HCM-causing troponin T mutations defines the degree of myofilament dysfunction in human cardiomyocytes, J Mol Cell Cardiol 150 (2021) 77–90. [PubMed: 33148509]

[7]. Poggesi C, Tesi C, Stehle R, Sarcomeric determinants of striated muscle relaxation kinetics, Pflugers Arch 449(6) (2005) 505–17. [PubMed: 15750836]

[8]. Piroddi N, Belus A, Scellini B, Tesi C, Giunti G, Cerbai E, Mugelli A, Poggesi C, Tension generation and relaxation in single myofibrils from human atrial and ventricular myocardium, Pflugers Arch 454(1) (2007) 63–73. [PubMed: 17123098]

[9]. Kreutziger KL, Piroddi N, McMichael JT, Tesi C, Poggesi C, Regnier M, Calcium binding kinetics of troponin C strongly modulate cooperative activation and tension kinetics in cardiac muscle, J Mol Cell Cardiol 50(1) (2011) 165–74. [PubMed: 21035455]

[10]. Martins AS, Parvatiyar MS, Feng HZ, Bos JM, Gonzalez-Martinez D, Vukmirovic M, Turna RS, Sanchez-Gonzalez MA, Badger CD, Zorio DAR, Singh RK, Wang Y, Jin JP, Ackerman MJ, Pinto JR, In Vivo Analysis of Troponin C Knock-In (A8V) Mice: Evidence that TNNC1 Is a Hypertrophic Cardiomyopathy Susceptibility Gene, Circ Cardiovasc Genet 8(5) (2015) 653–664. [PubMed: 26304555]

[11]. Tardiff JC, Hewett TE, Palmer BM, Olsson C, Factor SM, Moore RL, Robbins J, Leinwand LA, Cardiac troponin T mutations result in allele-specific phenotypes in a mouse model for hypertrophic cardiomyopathy, J Clin Invest 104(4) (1999) 469–81. [PubMed: 10449439]

[12]. Wang L, Kim K, Parikh S, Cadar AG, Bersell KR, He H, Pinto JR, Kryshtal DO, Knollmann BC, Hypertrophic cardiomyopathy-linked mutation in troponin T causes myofibrillar disarray and pro-arrhythmic action potential changes in human iPSC cardiomyocytes, J Mol Cell Cardiol 114 (2018) 320–327. [PubMed: 29217433]

[13]. Wang Y, Pinto JR, Solis RS, Dweck D, Liang J, Diaz-Perez Z, Ge Y, Walker JW, Potter JD, Generation and functional characterization of knock-in mice harboring the cardiac troponin I-R21C mutation associated with hypertrophic cardiomyopathy, J Biol Chem 287(3) (2012) 2156–67. [PubMed: 22086914]

[14]. Anderson RL, Trivedi DV, Sarkar SS, Henze M, Ma W, Gong H, Rogers CS, Gorham JM, Wong FL, Morck MM, Seidman JG, Ruppel KM, Irving TC, Cooke R, Green EM, Spudich JA, Deciphering the super relaxed state of human beta-cardiac myosin and the mode of action of mavacamten from myosin molecules to muscle fibers, Proc Natl Acad Sci U S A 115(35) (2018) E8143–E8152. [PubMed: 30104387]

[15]. McNamara JW, Li A, Dos Remedios CG, Cooke R, The role of super-relaxed myosin in skeletal and cardiac muscle, Biophys Rev 7(1) (2015) 5–14. [PubMed: 28509977]

[16]. Korte FS, Feest ER, Razumova MV, Tu AY, Regnier M, Enhanced Ca^{2+} binding of cardiac troponin reduces sarcomere length dependence of contractile activation independently of strong crossbridges, Am J Physiol Heart Circ Physiol 303(7) (2012) H863–70. [PubMed: 22865385]

[17]. Wang D, Robertson IM, Li MX, McCully ME, Crane ML, Luo Z, Daggett A.Y. Tu V., Sykes BD, Regnier M, Structural and functional consequences of the cardiac troponin C L48Q Ca(2+)-sensitizing mutation, Biochemistry 51(22) (2012) 4473–87. [PubMed: 22591429]

[18]. Wang D, McCully ME, Luo Z, McMichael J, Tu AY, Daggett V, Regnier M, Structural and functional consequences of cardiac troponin C L57Q and I61Q Ca(2+)-desensitizing variants, Arch Biochem Biophys 535(1) (2013) 68–75. [PubMed: 23454346]

[19]. Tikunova SB, Liu B, Swindle N, Little SC, Gomes AV, Swartz DR, Davis JP, Effect of calcium-sensitizing mutations on calcium binding and exchange with troponin C in increasingly complex biochemical systems, Biochemistry 49(9) (2010) 1975–84. [PubMed: 20128626]

[20]. Feest ER, Steven Korte F, Tu AY, Dai J, Razumova MV, Murry CE, Regnier M, Thin filament incorporation of an engineered cardiac troponin C variant (L48Q) enhances contractility in intact cardiomyocytes from healthy and infarcted hearts, J Mol Cell Cardiol 72 (2014) 219–27. [PubMed: 24690333]

[21]. Powers JD, Kooiker KB, Mason AB, Teitgen AE, Flint GV, Tardiff JC, Schwartz SD, McCulloch AD, Regnier M, Davis J, Moussavi-Harami F, Modulating the tension-time integral of the cardiac twitch prevents dilated cardiomyopathy in murine hearts, JCI Insight 5(20) (2020) e142446: 1–13.

[22]. Davis JP, Shettigar V, Tikunova SB, Little SC, Liu B, Siddiqui JK, Janssen PM, Ziolo MT, Walton SD, Designing proteins to combat disease: Cardiac troponin C as an example, Arch Biochem Biophys 601 (2016) 4–10. [PubMed: 26901433]

[23]. Mijailovich SM, Prodanovic M, Vasovic L, Stojanovic B, Maric M, Prodanovic D, Powers J, Davis J, Geeves M, Regnier M, Modulation of Calcium Sensitivity and Twitch Contractions in Cardiac Muscle with Troponin-C Mutations: Simulations and Experiments, Biophysical Journal 116(3) (2019) 116a.

[24]. Prodanovic M, Stojanovic B, Maric M, Prodanovic D, M.S. M, Tuning cooperativity of calcium activation in cardiac muscle, in: Tsihrintza GA, Virvou M, Jain LC (Eds.) Computational Bioengineering and Bioinformatics. Learning and Analytics in Intelegent Systems, Springer, Cham, 2020, pp. Vol. 11: 27–42.

[25]. Chase PB, Macpherson JM, Daniel TL, A spatially explicit nanomechanical model of the half-sarcomere: myofilament compliance affects Ca(2+)-activation, Ann Biomed Eng 32(11) (2004) 1559–68. [PubMed: 15636115]

[26]. Tanner BC, Daniel TL, Regnier M, Filament compliance influences cooperative activation of thin filaments and the dynamics of force production in skeletal muscle, PLoS Comput Biol 8(5) (2012) e1002506.

[27]. Tanner BC, Regnier M, Daniel TL, A spatially explicit model of muscle contraction explains a relationship between activation phase, power and ATP utilization in insect flight, J Exp Biol 211(Pt 2) (2008) 180–6. [PubMed: 18165245]

[28]. Mijailovich SM, Kayser-Herold O, Stojanovic B, Nedic D, Irving TC, Geeves MA, Three-dimensional stochastic model of actin-myosin binding in the sarcomere lattice, J Gen Physiol 148(6) (2016) 459–488. [PubMed: 27864330]

[29]. Mijailovich SM, Stojanovic B, Nedic D, Svicevic M, Geeves MA, Irving TC, Granzier H, Nebulin and Titin Modulate Crossbridge Cycling and Length Dependent Calcium Sensitivity J Gen Physiol 151(5) (2019) 680–704. [PubMed: 30948421]

[30]. Irving M, Regulation of Contraction by the Thick Filaments in Skeletal Muscle, Biophys J 113(12) (2017) 2579–2594. [PubMed: 29262355]

[31]. Brunello E, Fusi L, Ghisleni A, Park-Holohan SJ, Ovejero JG, Narayanan T, Irving M, Myosin filament-based regulation of the dynamics of contraction in heart muscle, Proc Natl Acad Sci U S A 117(14) (2020) 8177–8186. [PubMed: 32220962]

[32]. Geeves M, Griffiths H, Mijailovich S, Smith D, Cooperative [Ca(2)+]-dependent regulation of the rate of myosin binding to actin: solution data and the tropomyosin chain model, Biophys J 100(11) (2011) 2679–87. [PubMed: 21641313]

[33]. Mijailovich SM, Kayser-Herold O, Li X, Griffiths H, Geeves MA, Cooperative regulation of myosin-S1 binding to actin filaments by a continuous flexible Tm-Tn chain, Eur Biophys J 41(12) (2012) 1015–32. [PubMed: 23052974]

[34]. Robinson TF, Winegrad S, Variation of thin filament length in heart muscles, Nature 267(5606) (1977) 74–5. [PubMed: 859640]

[35]. Huxley HE, Stewart A, Sosa H, Irving T, X-ray diffraction measurements of the extensibility of actin and myosin filaments in contracting muscle, Biophys J 67(6) (1994) 2411–21. [PubMed: 7696481]

[36]. Wakabayashi K, Sugimoto Y, Tanaka H, Ueno Y, Takezawa Y, Amemiya Y, X-ray diffraction evidence for the extensibility of actin and myosin filaments during muscle contraction, Biophys J 67(6) (1994) 2422–35. [PubMed: 7779179]

[37]. Prodanovic M, Irving TC, Mijailovich SM, X-ray diffraction from nonuniformly stretched helical molecules, J Appl Crystallogr 49(Pt 3) (2016) 784–797. [PubMed: 27275136]

[38]. Luther PK, Bennett PM, Knupp C, Craig R, Padron R, Harris SP, Patel J, Moss RL, Understanding the organisation and role of myosin binding protein C in normal striated muscle

by comparison with MyBP-C knockout cardiac muscle, J Mol Biol 384(1) (2008) 60–72. [PubMed: 18817784]

[39]. Irving TC, Konhilas J, Perry D, Fischetti R, de Tombe PP, Myofilament lattice spacing as a function of sarcomere length in isolated rat myocardium, Am J Physiol Heart Circ Physiol 279(5) (2000) H2568–73. [PubMed: 11045995]

[40]. Williams CD, Salcedo MK, Irving TC, Regnier M, Daniel TL, The length-tension curve in muscle depends on lattice spacing, Proc Biol Sci 280(1766) (2013) 20130697.

[41]. Kojima H, Ishijima A, Yanagida T, Direct measurement of stiffness of single actin filaments with and without tropomyosin by in vitro nanomanipulation, Proc Natl Acad Sci U S A 91(26) (1994) 12962–6. [PubMed: 7809155]

[42]. Caremani M, Pinzauti F, Reconditi M, Piazzesi G, Stienen GJ, Lombardi V, Linari M, Size and speed of the working stroke of cardiac myosin in situ, Proc Natl Acad Sci U S A 113(13) (2016) 3675–80. [PubMed: 26984499]

[43]. Linari M, Dobbie I, Reconditi M, Koubassova N, Irving M, Piazzesi G, Lombardi V, The stiffness of skeletal muscle in isometric contraction and rigor: the fraction of myosin heads bound to actin, Biophys J 74(5) (1998) 2459–73. [PubMed: 9591672]

[44]. Schaper J, Meiser E, Stammler G, Ultrastructural morphometric analysis of myocardium from dogs, rats, hamsters, mice, and from human hearts, Circ Res 56(3) (1985) 377–91. [PubMed: 3882260]

[45]. Barth E, Stammler G, Speiser B, Schaper J, Ultrastructural quantitation of mitochondria and myofilaments in cardiac muscle from 10 different animal species including man, J Mol Cell Cardiol 24(7) (1992) 669–81. [PubMed: 1404407]

[46]. Janssen PM, Stull LB, Marban E, Myofilament properties comprise the rate-limiting step for cardiac relaxation at body temperature in the rat, Am J Physiol Heart Circ Physiol 282(2) (2002) H499–507. [PubMed: 11788397]

[47]. Ferrantini C, Coppini R, Scellini B, Ferrara C, Pioner JM, Mazzoni L, Priori S, Cerbai E, Tesi C, Poggesi C, R4496C RyR2 mutation impairs atrial and ventricular contractility, J Gen Physiol 147(1) (2016) 39–52. [PubMed: 26666913]

[48]. Ferrantini C, Coppini R, Sacconi L, Tosi B, Zhang ML, Wang GL, de Vries E, Hoppenbrouwers E, Pavone F, Cerbai E, Tesi C, Poggesi C, ter Keurs HE, Impact of detubulation on force and kinetics of cardiac muscle contraction, J Gen Physiol 143(6) (2014) 783–97. [PubMed: 24863933]

[49]. Schiaffino S, Reggiani C, Molecular diversity of myofibrillar proteins: gene regulation and functional significance, Physiol Rev 76(2) (1996) 371–423. [PubMed: 8618961]

[50]. Fitzsimons DP, Patel JR, Moss RL, Role of myosin heavy chain composition in kinetics of force development and relaxation in rat myocardium, J Physiol 513 (Pt 1) (1998) 171–83. [PubMed: 9782168]

[51]. Cappelli V, Bottinelli R, Poggesi C, Moggio R, Reggiani C, Shortening velocity and myosin and myofibrillar ATPase activity related to myosin isoenzyme composition during postnatal development in rat myocardium, Circ Res 65(2) (1989) 446–57. [PubMed: 2526695]

[52]. Woulfe KC, Ferrara C, Pioner JM, Mahaffey JH, Coppini R, Scellini B, Ferrantini C, Piroddi N, Tesi C, Poggesi C, Jeong M, A Novel Method of Isolating Myofibrils From Primary Cardiomyocyte Culture Suitable for Myofibril Mechanical Study, Front Cardiovasc Med 6 (2019) 12. [PubMed: 30838216]

[53]. Alpert NR, Brosseau C, Federico A, Krenz M, Robbins J, Warshaw DM, Molecular mechanics of mouse cardiac myosin isoforms, Am J Physiol Heart Circ Physiol 283(4) (2002) H1446–54. [PubMed: 12234796]

[54]. Regnier M, Rivera AJ, Chen Y, Chase PB, 2-deoxy-ATP enhances contractility of rat cardiac muscle, Circulation research 86(12) (2000) 1211–7. [PubMed: 10864910]

[55]. Malmqvist UP, Aronshtam A, Lowey S, Cardiac myosin isoforms from different species have unique enzymatic and mechanical properties, Biochemistry 43(47) (2004) 15058–65. [PubMed: 15554713]

[56]. Pellegrino MA, Canepari M, Rossi R, D'Antona G, Reggiani C, Bottinelli R, Orthologous myosin isoforms and scaling of shortening velocity with body size in mouse, rat, rabbit and human muscles, J Physiol 546(Pt 3) (2003) 677–89. [PubMed: 12562996]

[57]. Janssen PM, de Tombe PP, Uncontrolled sarcomere shortening increases intracellular Ca^{2+} transient in rat cardiac trabeculae, Am J Physiol 272(4 Pt 2) (1997) H1892–7. [PubMed: 9139976]

[58]. Swartz DR, Moss RL, Greaser ML, Characteristics of troponin C binding to the myofibrillar thin filament: extraction of troponin C is not random along the length of the thin filament, Biophys J 73(1) (1997) 293–305. [PubMed: 9199794]

[59]. Yang Z, Yamazaki M, Shen QW, Swartz DR, Differences between cardiac and skeletal troponin interaction with the thin filament probed by troponin exchange in skeletal myofibrils, Biophys J 97(1) (2009) 183–94. [PubMed: 19580756]

[60]. Hershberger RE, Hedges DJ, Morales A, Dilated cardiomyopathy: the complexity of a diverse genetic architecture, Nat Rev Cardiol 10(9) (2013) 531–47. [PubMed: 23900355]

[61]. Davis JP, Norman C, Kobayashi T, Solaro RJ, Swartz DR, Tikunova SB, Effects of thin and thick filament proteins on calcium binding and exchange with cardiac troponin C, Biophys J 92(9) (2007) 3195–206. [PubMed: 17293397]

[62]. Wang YP, Fuchs F, Length, force, and Ca(2+)-troponin C affinity in cardiac and slow skeletal muscle, Am J Physiol 266(4 Pt 1) (1994) C1077–82. [PubMed: 8178954]

[63]. Fuchs F, Martyn DA, Length-dependent Ca(2+) activation in cardiac muscle: some remaining questions, J Muscle Res Cell Motil 26(4–5) (2005) 199–212. [PubMed: 16205841]

[64]. Smith L, Tainter C, Regnier M, Martyn DA, Cooperative cross-bridge activation of thin filaments contributes to the Frank-Starling mechanism in cardiac muscle, Biophys J 96(9) (2009) 3692–702. [PubMed: 19413974]

[65]. Duke TA, Molecular model of muscle contraction, Proc Natl Acad Sci U S A 96(6) (1999) 2770–5. [PubMed: 10077586]

[66]. Smith DA, Geeves MA, Cooperative regulation of myosin-actin interactions by a continuous flexible chain II: actin-tropomyosin-troponin and regulation by calcium., Biophys. J. 84 (2003) 3168–80. [PubMed: 12719246]

[67]. Poole KJ, Lorenz M, Evans G, Rosenbaum G, Pirani A, Craig R, Tobacman LS, Lehman W, Holmes KC, A comparison of muscle thin filament models obtained from electron microscopy reconstructions and low-angle X-ray fibre diagrams from non-overlap muscle, J Struct Biol 155(2) (2006) 273–84. [PubMed: 16793285]

[68]. Pirani A, Xu C, Hatch V, Craig R, Tobacman LS, Lehman W, Single particle analysis of relaxed and activated muscle thin filaments, J Mol Biol 346(3) (2005) 761–72. [PubMed: 15713461]

[69]. Robinson TF, Winegrad S, The measurement and dynamic implications of thin filament lengths in heart muscle, J Physiol 286 (1979) 607–19. [PubMed: 312321]

[70]. Irving TC, Maughan DW, In vivo x-ray diffraction of indirect flight muscle from Drosophila melanogaster, Biophys J 78(5) (2000) 2511–5. [PubMed: 10777748]

[71]. Deacon JC, Bloemink MJ, Rezavandi H, Geeves MA, Leinwand LA, Identification of functional differences between recombinant human alpha and beta cardiac myosin motors, Cell Mol Life Sci 69(13) (2012) 2261–77. [PubMed: 22349210]

[72]. Deacon JC, Bloemink MJ, Rezavandi H, Geeves MA, Leinwand LA, Erratum to: Identification of functional differences between recombinant human alpha and beta cardiac myosin motors, Cell Mol Life Sci 69(24) (2012) 4239–55. [PubMed: 23001010]

[73]. Mijailovich SM, Nedic D, Svicevic M, Stojanovic B, Walklate J, Ujfalusi Z, Geeves MA, Modeling the Actin.myosin ATPase Cross-Bridge Cycle for Skeletal and Cardiac Muscle Myosin Isoforms, Biophys J 112(5) (2017) 984–996. [PubMed: 28297657]

Highlights

- Familial cardiac diseases usually originate from mutations in sarcomeric proteins
- The L48Q and I61Q mutations in cTnC modulate the release rate of Ca^{2+} from cTnC
- The effects of the cTnC mutations are evaluated by *in silico* simulations
- Twitch contractions in L48Q trabeculae have slower relaxation than WT
- Twitches in I61Q trabeculae have markedly reduced peak tension comparing to WT
- An explicit 3-D model predicts the effects of variable incorporation of mutations
- The approach is suitable for the study on mutations in any major sarcomeric protein

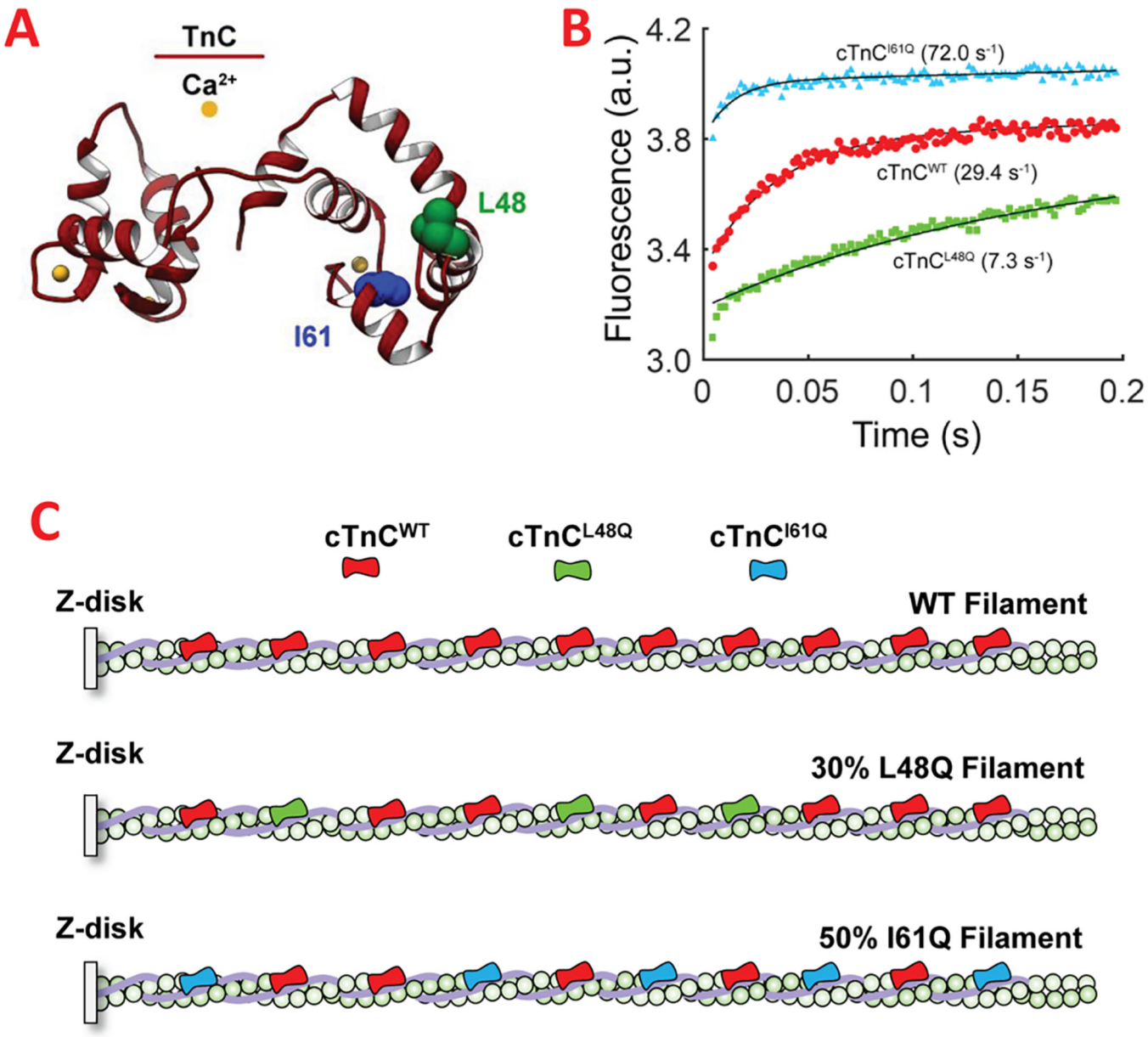

Figure 1.

Experimental design to use the MUSICO spatially explicit model with experimentally determined properties of TnC mutations. (A) Two individual single point mutations in cTnC that result in a Glutamine (Q) substitution at either position Leu48 (*green*) or Ile61 (*blue*) were examined. The Ca^{2+} affinity of each cTnC mutation was previously determined [9] and was dependent of the Ca^{2+} dissociation rate k_{-Ca} from the cTn complex, measured using stopped-flow spectrophotometry (B). These rates were incorporated into the model at individual cTnC subunits along the thin filaments (C), allowing the investigation of the effects of mutation incorporation (30% $cTnC^{L48Q}$ and 50% $cTnC^{I61Q}$) and spatial distribution on twitch tension and kinetics.

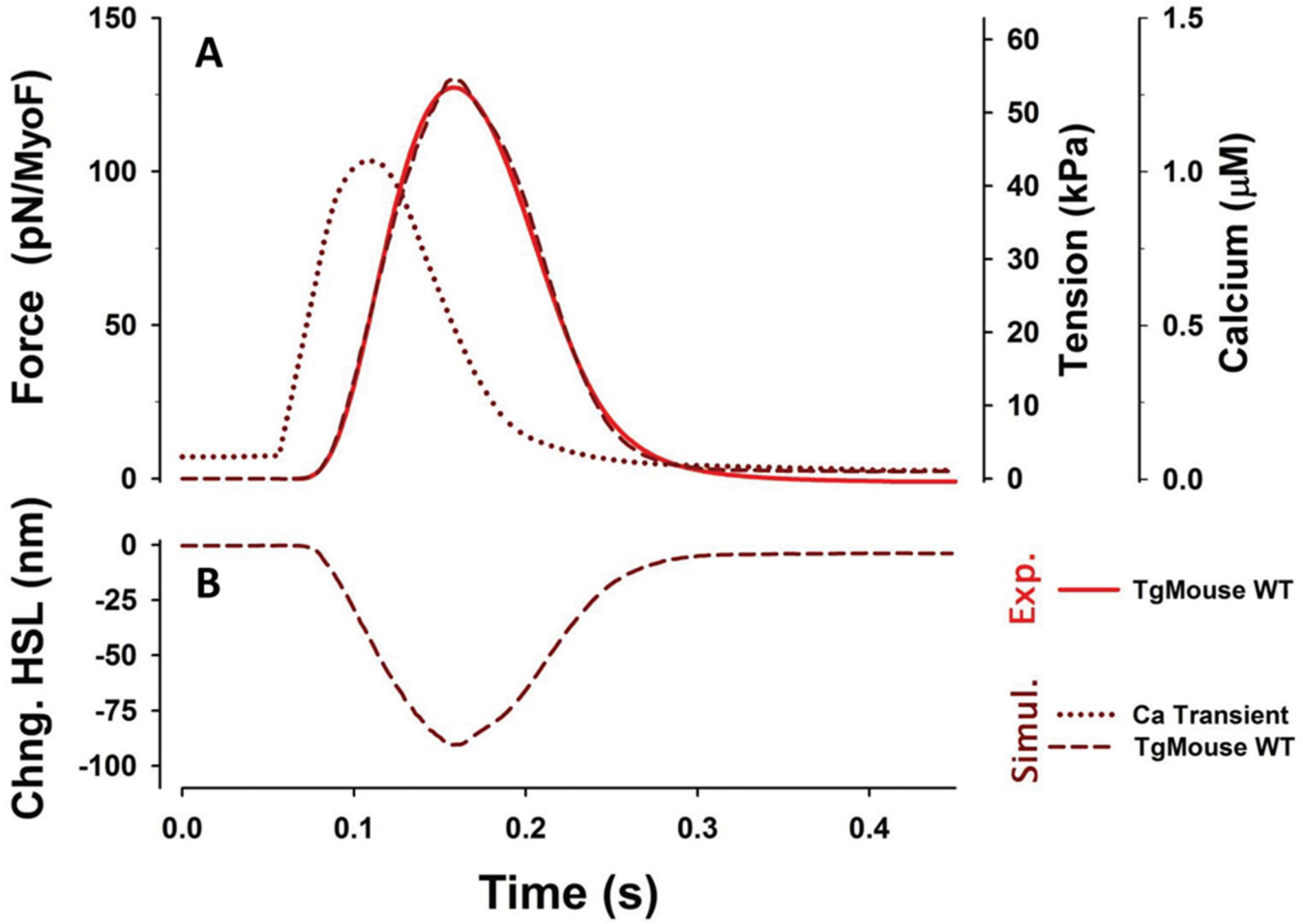

Figure 2.

The predicted twitch tension transient and change in half sarcomere length (Chng. HSL) in WT transgenic mouse (TgMouse) trabecula (*dark red dashed lines*). (A) The [Ca^{2+}] transient for mouse myocyte contraction at 30 °C (*dark red dotted line*) was derived from the observed peak [Ca^{2+}], basal level and decay time observed in mice by Davis et al. [1], scaled to the shape of the transient [Ca^{2+}] measurements in rat trabeculae [46]; the tension transients in mouse trabeculae were also observed at 30 °C (*red solid line*). (B) Predicted change in half sarcomere length (HSL) during twitch contraction in fixed length trabecula.

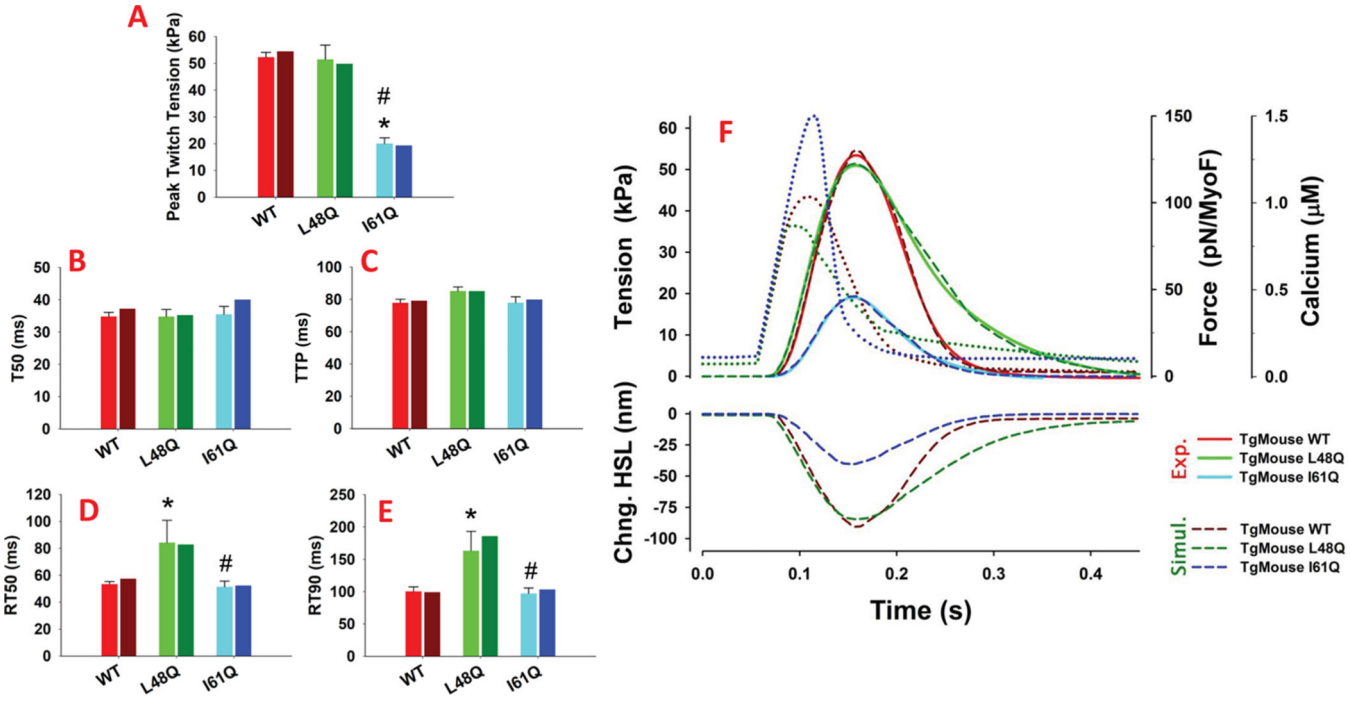

Figure 3.

Average observed values for twitch contractions for WT, I61Q and L48Q trabeculae from transgenic mice (TgMouse) compared to MUSICO predictions. Experimental values (A-E) represent the Mean + S.E.M. (N for WT = 4; N for I61Q = 9; N for L48Q = 5). *p < 0.05 for each variant versus WT and #p < 0.05 for I61Q versus L48Q using a one-way ANOVA with a Tukey post-hoc test of significance. The bar graphs show peak tension (Tp, A), time to 50% (B), 100% Tp (C), and relaxation time (RT) to loss of 50% (D) and 90% (E) of peak tension. (F) MUSICO predictions of twitches for WT and transgenic mice trabeculae at sarcomere length 2.3 μm (*dashed lines*) superimposed on the observed twitches (*solid lines*) for WT (*red*), L48Q (*green*) and I61Q (*blue*). Best fit parameters are listed in Table 3. The twitches are driven by the Ca^{2+} transients (*dotted lines*) from Davis et al. [1], and model estimates of half sarcomere length changes (Chng. HSL).

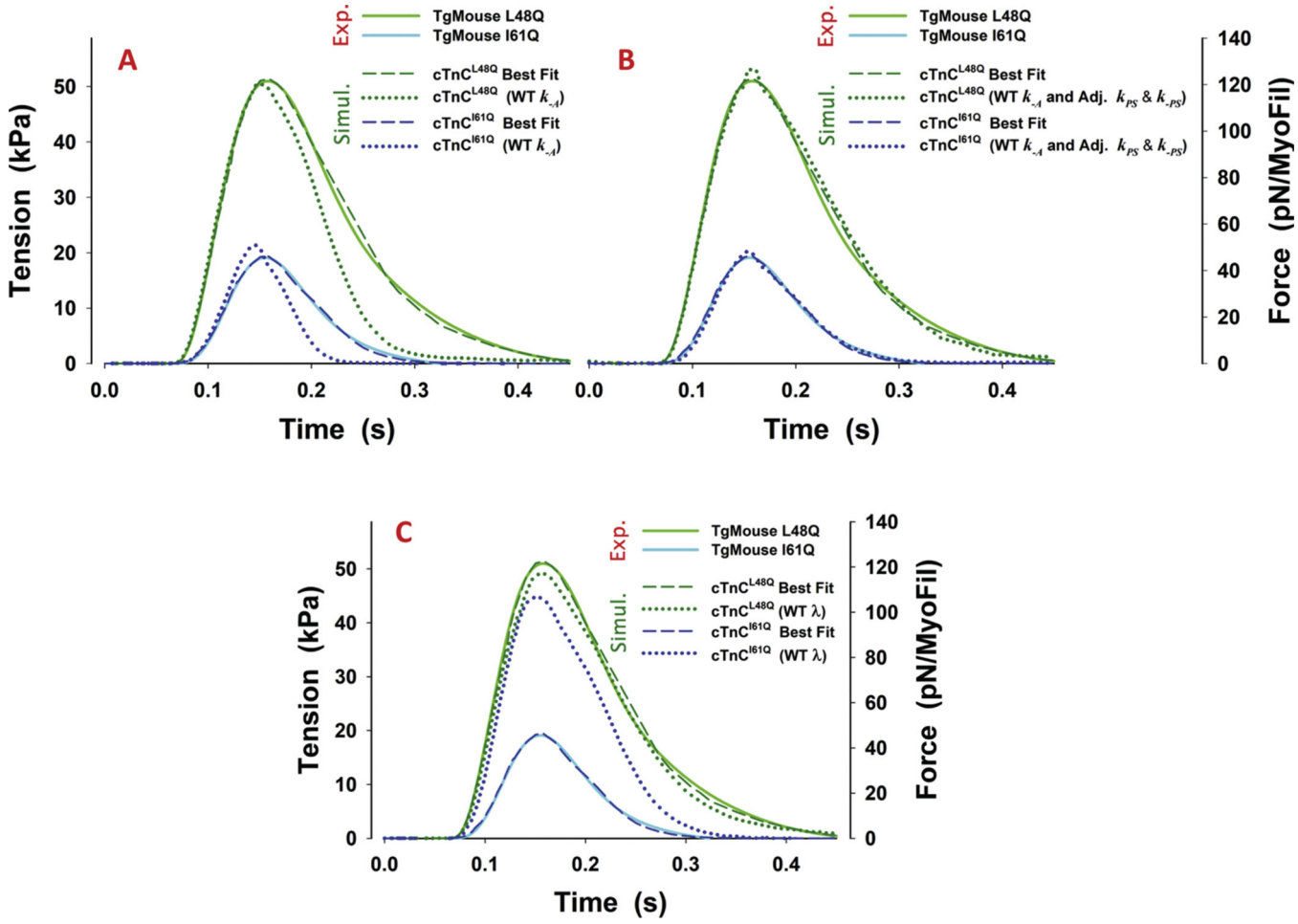

Figure 4.

The tension transients and the best fits from Fig. 3F are replotted with A) the resulting transient for simulations of transgenic trabeculae containing cTnC^{L48Q} and cTnC^{I61Q} if the value of k^{o}_{-A} is the same as for WT (=115 s^{-1}) (*dotted lines*); B) Restoring the observed tension transient of L48Q and I61Q trabeculae, from simulated the transients in (A) where of k^{o}_{-A} is set to value used in WT, by adjusting the values of k_{PS} and k_{-PS} by setting $k^{\max}_{PS}$ and k_{-PS} to 100 and 50 s^{-1} for cTnC^{L48Q}, 60 and 30 s^{-1} for cTnC^{I61Q}.C) The resulting transient if λ is the same as for the WT (=10) (*dotted lines*).

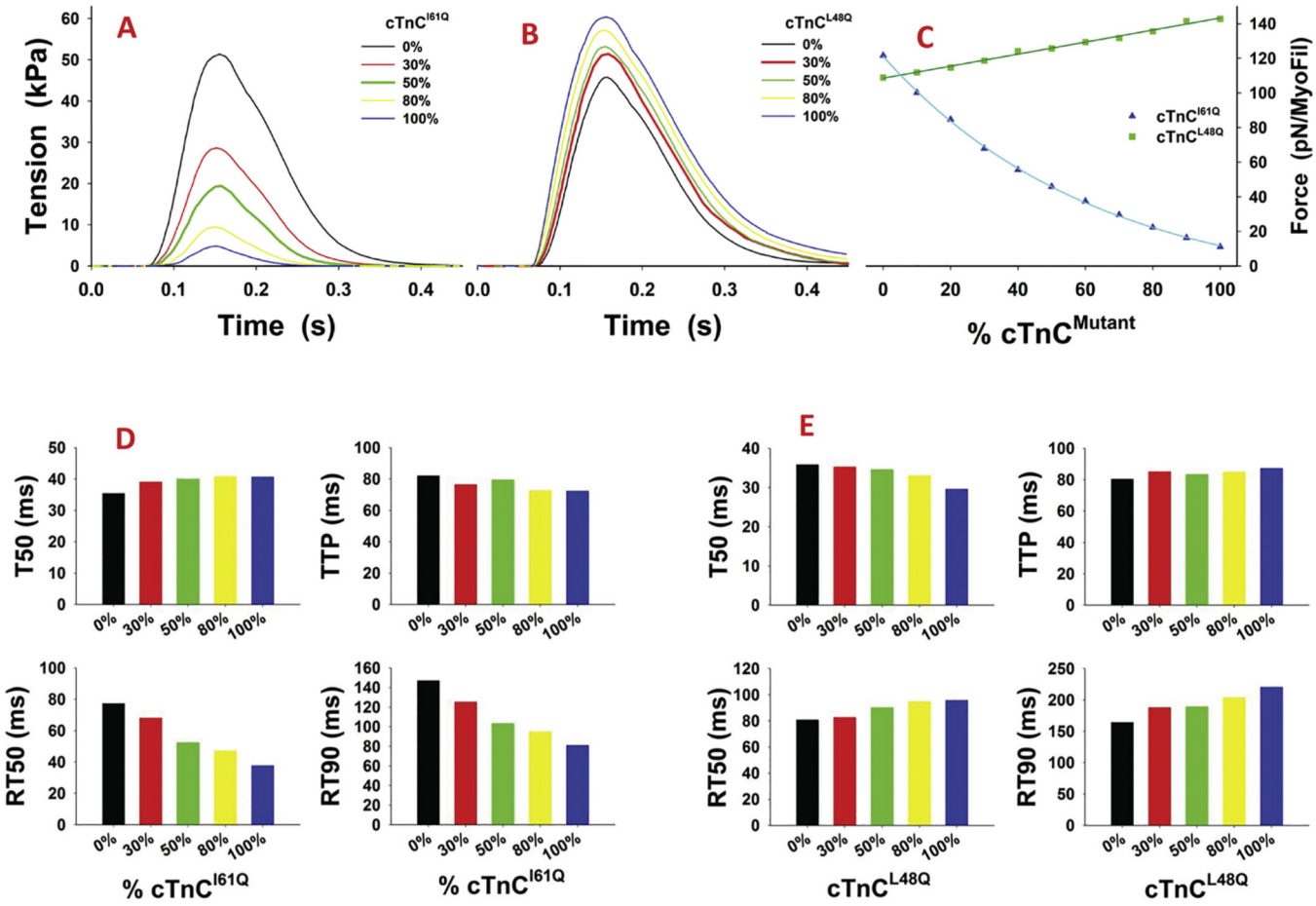

Figure 5.

Predicted effect of % incorporation of $cTnC^{I61Q}$ (A) and $cTnC^{L48Q}$ (B) on twitches. C) Peak tension as a function of % incorporation (Δ) $cTnC^{I61Q}$, (□) $cTnC^{L48Q}$. The bar graphs show time to 50% (T50), 100% (TPP) of peak tension, and relaxation time to loss of 50% (RT50) and 90% (RT50) of peak tension for $cTnC^{I61Q}$ (D) and for $cTnC^{L48Q}$ (E).

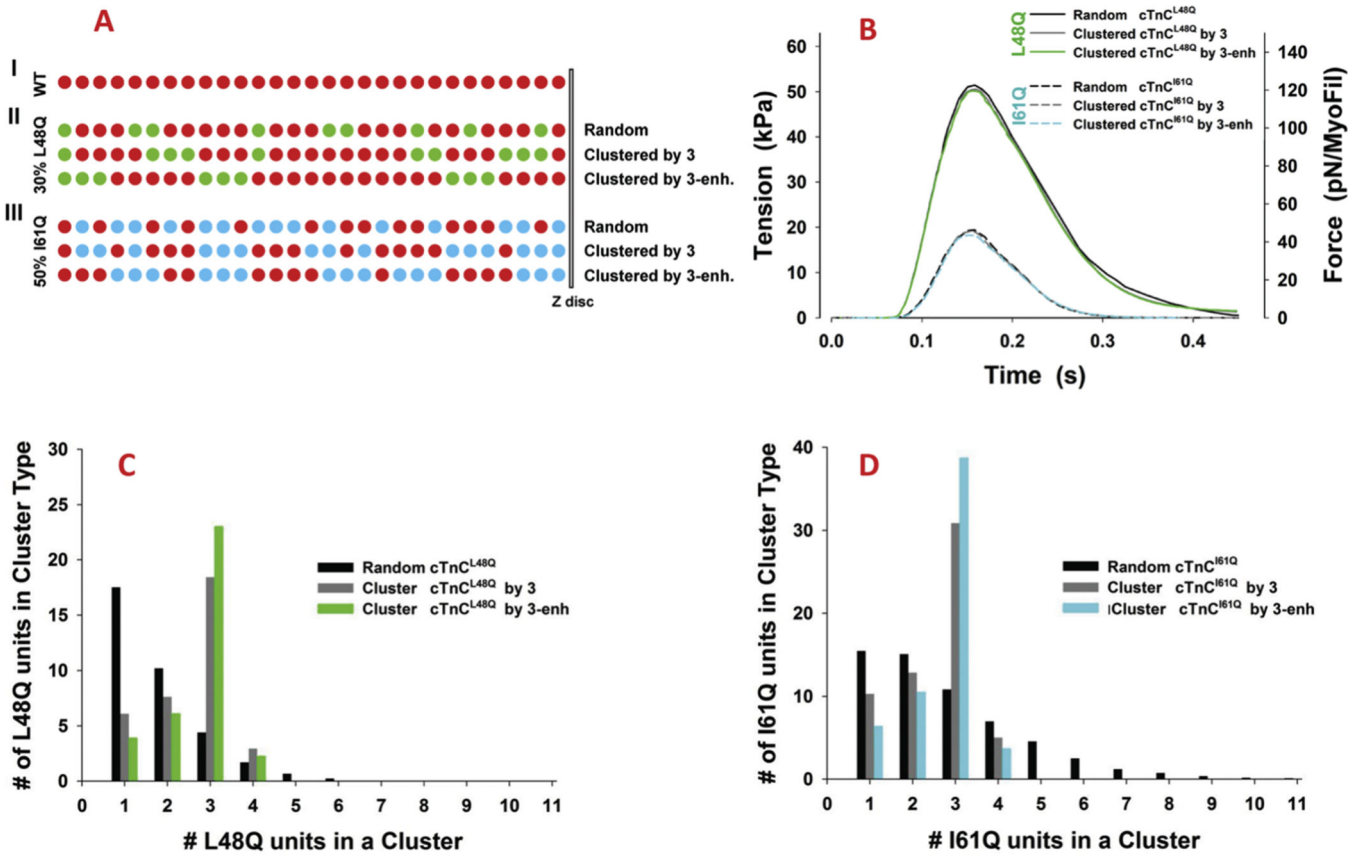

Figure 6.

The effect of clustering of mutated TnC in each actin filament. A) Different random distributions of mutant TnC within a representative strand of an actin filaments if mutant TnCs tend to cluster: I. $cTnC^{WT}$, II. random and clustered distributions of 30% $cTnC^{L48Q}$ and III. random and clustered distributions of 50% $cTnC^{I61Q}$. In II and III the distribution includes a significant number of clusters of three mutated cTnCs, denoted as “Clusters by 3” and further enhanced number of the clusters of three, by ~ 25%, denoted as “Clusters by 3-enh.” B) The effect of mutant cTnC distributions on tension transients where the random distribution simulation data (from Fig. 2B) is compared with clustering $cTnC^{L48Q}$ (*solid lines*) and $cTnC^{I61Q}$ (*dotted lines*) by 3 or by 3-enh, keeping partitioning as shown in (A). Clustering distributions on $cTnC^{I61Q}$ (C) and $cTnC^{L48Q}$ (D) represented as number of mutant units in each cluster group per actin filament keeping level of overall incorporation as shown in (A).

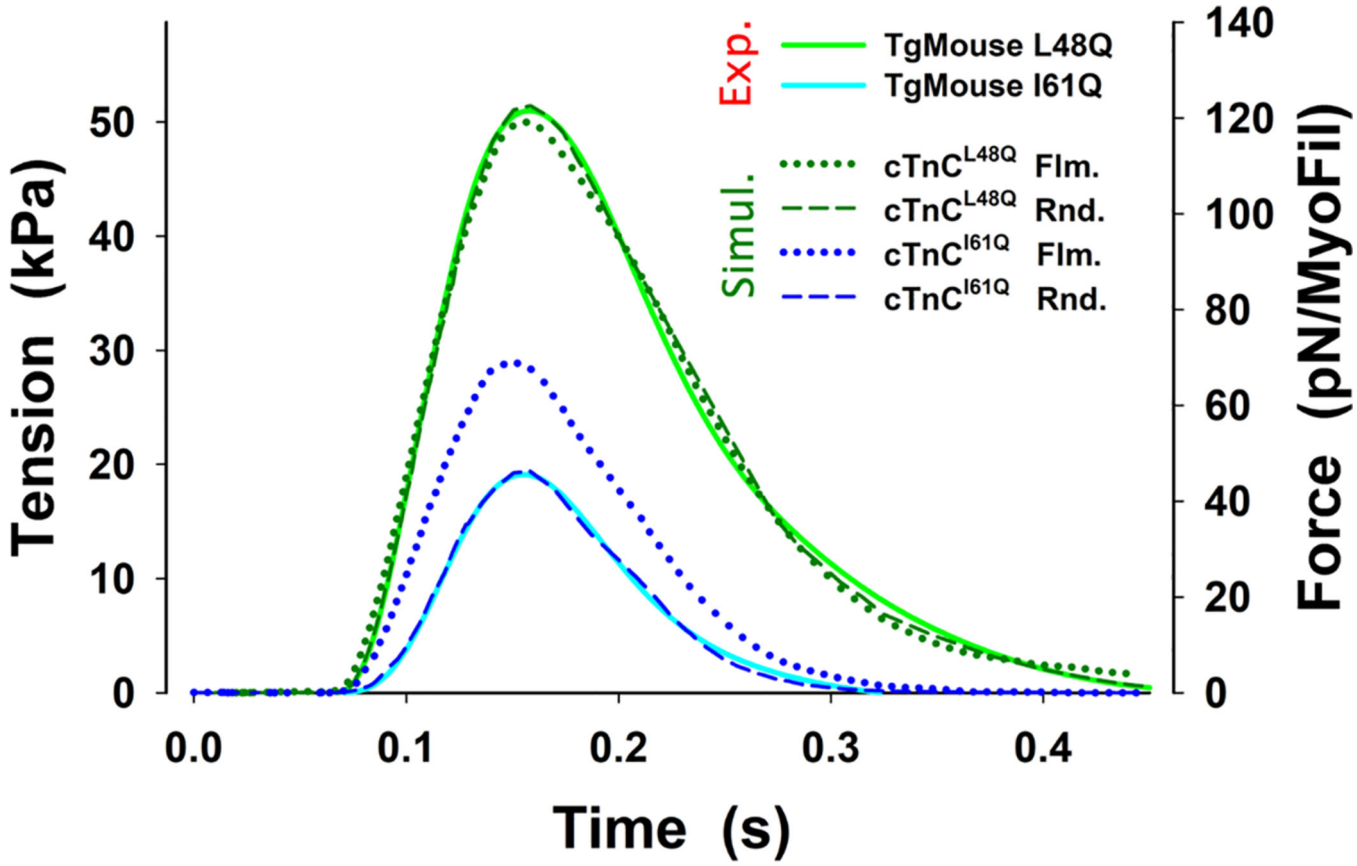

Figure 7.

The effect of the distributions of cTnC mutations, where $cTnC^{WT}$ and $cTnC^{L48Q}$ (or $cTnC^{I61Q}$) are segregated into separate thin filaments (Flm.), or they are randomly distributed along each thin filament (Rnd.). In each $cTnC^{L48Q}$ simulation incorporation of the mutation was 30% and for $cTnC^{I61Q}$ was 50%. Tension observed transients (*solid lines*) and the best fits from Fig. 3F with the mutant cTnC distributed at random along each filament (*dashed lines*), are compared with thin filaments containing only WT or only mutant cTnCs randomly distributed within the sarcomere (*dotted lines*).

Table 1.

MUSICO parameters for the simulations of twitch contractions in intact mice trabeculae at fixed length and at temperature 30 °C.

Description	Parameter	Iso Trabeculae
Crossbridge Cycle		
Myosin-actin binding rate	k^{o}_{+A}	350s^{-1}
Myosin-actin detachment rate[a]	k^{o}_{-A}	115 s^{-}
Myosin stroke cap rate[b]	k^{cap}_{+pi}	10000 s^{-1}
Myosin reverse stroke cap rate[b]	k^{cap}_{-pi}	1000 s^{-1}
Power stroke Gibbs energy change [2,28,29]	G_{stroke}	−13k$_s$T
Working stroke [2,28,29,65]	d	10.5 nm
Second working stroke [2,28,29]	δ	1 nm
ADP release rate*	k^{o}_{+D}	500 s^{-1}
ATP binding and myosin detachment[a]	k_{+T}	10^6 s^{-1}
Hydrolysis forward rate[a]	k_{+H}	240 s^{-1}
Hydrolysis backward rate[a]	k_{-H}	24 s^{-1}
Crossbridge stiffness [2,28,29,65]	κ	1.3 pN/nm
k_BT at 30 °C	k_BT	4.185 pN·nm
Calcium Kinetics		
Calcium binding to TnC equilib. rate [32,66]	$\bar{K}_{Ca}$	10^6 M^{-1}
Calcium binding rate to TnC [32,66]	$\bar{k}_{ca}$	7.54–10^7 M^{-1}·s^{-1}
Calcium dissociation rate from TnC [9,17,18]	k_{-Ca}	75.4·10^7 M^{-1}·s^{-1}
TnI-actin equilibrium rate const. at high Ca^{2+}	λ	10
TnI-actin backward rate const.	λ_{-}	375 s^{-1}
TnI-actin-Ca cooperativity coefficient [32,66]	ε_o	0.01
CFC		
Tropomyosin pinning angle [67]	φ_{-}	−25°
Myosin Tin angular displacement [67]	φ_{+}	10°
Angular SD of free CFC [33,68]	σ_0	29.7°
Persistence length of Tm-Tn conf. chain [33]	$1/\xi$	50 nm
Parked State		
Transition rate to “parked state”[c]	k_{-ps}	200 s^{-1}
Baseline rate[c]	k^{0}_{Ps}	5 s^{-1}

Description	Parameter	Iso Trabeculae
Crossbridge Cycle		
Amplitude[c]	k_{Ps}^{max}	400 s^{-1}
Calcium Hill function slope[c]	b	5
Half activation point of the Hill function[c]	$[Ca^{2+}]_{50}$	0.6 μM
Sarcomere		
Length of Sarcomere	SL	2.2 μm
Reference Length of Actin filament [34,69]	L_a^o	1.1 μm
Interfilament Spacing at SL=2.3 μm [70]	d_{10}	33.10 nm
Thin filament elastic modulus [35,41]	AE_a	65 nN
Thick filament elastic modulus [35]	AE_m	132 nN

[a]Based on mouse and human α muosin values in [71, 72], with corrections for temparature, ionic strength as documented in[73].

[b]The power stroke rates (k_{+Pi} an dk_{-Pi}) in mice are excepted to increase by the 1.5 to 3 comparing to rate [2] and this is achieved by increase of cap (rates (k_{+pi}^{cap} and k_{-pi}^{cap}) by factor 10.

[c]Assumed.

Table 2.

Comparison of parameters for the twitch contractions simulations between Rat (Janssen et al. [46] at 30 °C) and Mouse (Powers at 30 °C)

Description	Parameter	Rat	Mouse
Myosin-actin binding rate	k^{o}_{+A}	256 s^{-1}	350 s^{-1}
Myosin-actin detachment rate	k^{o}_{-A}	66 s^{-1}	115 s^{-1}
Myosin stroke cap rate	k^{cap}_{+pi}	1000 s^{-1}	10000 s^{-1}
ADP release rate	k^{o}_{+D}	92 s^{-1}	500 s^{-1}
Hydrolysis forward rate	k_{+H}	100 s^{-1}	240 s^{-1}
Hydrolysis backward rate	k_{-H}	10 s^{-1}	24 s^{-1}
Half activation of the transition rate from PS	$[Ca^{2+}]_{50}$	1 μM	0.6 μM
Length of sarcomere	SL	2.2 μm	2.3 μm

J Mol Cell Cardiol. Author manuscript; available in PMC 2021 June 29.

Table 3.

Differences between the fitted parameters used for twitches for WT and the two TnC mutations. The parameter adjustment for mutants L48Q and I61Q are obtained from simulations using random distribution of the mutants and WT TnCs in thin filaments for specified level of the mutant incorporation.

	Description	Parameter	WT	L48Q	I61Q
	Myosin-actin detachment rate		115 s^{-1}	80 s^{-1}	60 s^{-1}
Calcium Kinetics	Equilibrium const. of Ca^{2+} binding to TnC		10^6 M^{-1}	3.21–10^6 M^{-1}	3.17–10^5 M^{-1}
	Ca^{2+} dissociation rate const. from TnC		75.4 s^{-1}	23.52 s^{-1}	237.7 s^{-1}
	Equilibrium const. of TnI.Ca-actin interaction		10	20	1.365
	Incorporation [1]		0%	30%	50%